© 2024. Published by The Company of Biologists Ltd | Journal of Cell Science (2024) 137, jcs261639. doi:10.1242/jcs.261639

RESEARCH ARTICLE

Artificial tethering of constitutive centromere-associated network proteins induces CENP-A deposition without Knl2 in DT40 cells

JingHui Cao, Tetsuya Hori, Mariko Ariyoshi and Tatsuo Fukagawa*

ABSTRACT

The kinetochore is an essential structure for chromosome segregation. Although the kinetochore is usually formed on a centromere locus, it can be artificially formed at a non-centromere locus by protein tethering. An artificial kinetochore can be formed by tethering of CENP-C or CENP-I, members of the constitutive centromere-associated network (CCAN). However, how CENP-C or CENP-I recruit the centromere-specific histone CENP-A to form an artificial kinetochore remains unclear. In this study, we analyzed this issue using the tethering assay combined with an auxin-inducible degron (AID)-based knockout method in chicken DT40 cells. We found that tethering of CENP-C or CENP-I induced CENP-A incorporation at the non-centromeric locus in the absence of Knl2 (or MIS18BP1), a component of the Mis18 complex, and that Knl2 tethering recruited CENP-A in the absence of CENP-C. We also showed that CENP-C coimmunoprecipitated with HJURP, independently of Knl2. Considering these results, we propose that CENP-C recruits CENP-A by HJURP binding to form an artificial kinetochore. Our results suggest that CENP-C or CENP-I exert CENP-A recruitment activity, independently of Knl2, for artificial kinetochore formation in chicken DT40 cells. This gives us a new insight into mechanisms for CENP-A incorporation.

KEY WORDS: Centromere, Kinetochore, CENP-A, CENP-C, HJURP, Knl2

INTRODUCTION

The kinetochore is a large protein complex that bridges centromeric chromatin and spindle microtubules for accurate chromosome segregation during mitosis (Fukagawa and Earnshaw, 2014). The centromere, on which the kinetochore is formed, is specified at a particular locus on the chromosome via sequence-independent epigenetic mechanisms (Black and Cleveland, 2011; Fukagawa and Earnshaw, 2014). In this process, the centromere-specific histone H3 variant CENP-A plays a key epigenetic role because the formation of active centromeres in most species is triggered by CENP-A deposition into chromatin (Allshire and Karpen, 2008; Barnhart et al., 2011; Black and Cleveland, 2011; Fukagawa and Earnshaw, 2014; Guse et al., 2011; Mellone and Fachinetti, 2021; Mendiburo et al., 2011; Westhorpe and Straight, 2013). Therefore, addressing how CENP-A is specifically incorporated into centromeric chromatin is critical. In the current model, the Mis18 complex (Fujita et al., 2007; Hayashi et al., 2004; Maddox et al., 2007), containing Mis18α (or MIS18A), Mis18β (or OIP5) and Knl2 (MIS18BP1), associates with centromeric chromatin and then the CENP-A chaperone HJURP recognizes the Mis18 complex, which ensures correct CENP-A deposition from the HJURP–CENP-A–histone H4 complex onto centromeric chromatin (Nardi et al., 2016; Pan et al., 2017, 2019; Spiller et al., 2017; Subramanian et al., 2016). Using this cycle, the position of the centromere is maintained across generations. Therefore, many findings indicate that the Mis18 complex–HJURP pathway plays a major role in new CENP-A deposition (Pan et al., 2017, 2019; Spiller et al., 2017).

In parallel with these studies, we previously generated an artificial kinetochore by tethering kinetochore components to a non-centromeric locus in chicken DT40 cells using a LacO–LacI system (Hori et al., 2013). Similar tethering approaches have been used in various cells, including human and *Drosophila* cells (Barnhart et al., 2011; Gascoigne et al., 2011; Lacefield et al., 2009; Mendiburo et al., 2011; Palladino et al., 2020; Shono et al., 2015). In DT40 cells, we removed the original centromeric region to determine whether an artificial kinetochore could functionally replace the original kinetochore (Hori et al., 2013). Based on the functional assay, we generated two types of artificial kinetochores: one that did not contain CENP-A and one that did. In CENP-A-less artificial kinetochores, tethering proteins directly recruit the microtubule-binding Knl1–Mis12–Ndc80 (KMN) complex to a non-centromeric locus without constitutive centromere-associated network (CCAN) proteins (Hori et al., 2013). This type of artificial kinetochore is formed by tethering of the N-terminal domains of CENP-T and CENP-C into a non-centromeric locus. In another type of artificial kinetochore, CENP-A is incorporated near a non-centromeric LacO locus, and upon CENP-A incorporation into chromatin, most kinetochore components are recruited there to form a functional kinetochore. This type of kinetochore is formed by tethering of HJURP, Knl2, CENP-I or the CENP-C C-terminal fragment (Hori et al., 2013; Perpelescu et al., 2015). Similarly, tethering of CENP-C, CENP-I, HJURP and Knl2, as well as some chromatin-remodeling factors, recruits CENP-A to a non-centromeric locus in human cells (Shono et al., 2015). As HJURP and Knl2 are involved in the CENP-A deposition pathway in native centromeres, tethering of these proteins to the LacO locus should recruit CENP-A, which induces artificial kinetochore formation. However, how CENP-I or the C-terminal fragment of CENP-C recruits CENP-A to induce an artificial kinetochore at the non-centromeric LacO locus in chicken DT40 cells remains unclear. As CENP-C appears to associate with the Mis18 complex in human and mouse cells (Dambacher et al., 2012; McKinley and Cheeseman, 2014), CENP-C might recruit CENP-A via the Mis18 complex in these cells. However, Knl2 localization in G1 cells did not change in CENP-C-knockout chicken DT40 cells (Hori et al., 2017; Perpelescu et al., 2015), suggesting that the Mis18 complex does not associate with CENP-C during the G1 phase, when new CENP-A

Graduate School of Frontier Biosciences, Osaka University, Suita, Osaka 565-0871, Japan.

*Author for correspondence (fukagawa.tatsuo.fbs@osaka-u.ac.jp)

T.F., 0000-0001-8564-6852

Handling Editor: Renata Basto
Received 10 September 2023; Accepted 22 December 2023

Journal of Cell Science (2024) 137, jcs261639. doi:10.1242/jcs.261639

deposition occurs. Therefore, how CENP-C and CENP-I recruit CENP-A to a non-centromeric locus in chicken DT40 cells remains unclear.

Therefore, we aimed to address this question by combining a tethering assay with the auxin-inducible degron (AID)-based protein knockout method in chicken DT40 cells. We demonstrated that CENP-C or CENP-I recruits CENP-A in the absence of Knl2. We also demonstrated that CENP-C co-immunoprecipitated HJURP, independently of Knl2. Based on these results, we propose that CENP-C and CENP-I (via CENP-C) directly recruit HJURP for new CENP-A deposition.

RESULTS

Ectopic localization of inner kinetochore proteins causes efficient kinetochore formation at a non-centromeric locus

We summarize the kinetochore components used in this study and their possible roles in Fig. 1A. We confirmed whether the HJURP N-terminus [amino acids (aa) 1–400], Knl2 full-length (FL) (Knl2), CENP-C FL (CENP-C), CENP-C C-terminus (aa 601–864) and CENP-I FL (CENP-I) proteins induced artificial kinetochore formation at a non-centromeric locus in chicken DT40 cells (Fig. 1B,C). First, we inserted 256 copies of the LacO sequence at the end of the q-arm on chromosome Z in chicken DT40 cells, in which two loxP sequences are located across a native centromere on chromosome Z, and then expressed LacI-fused proteins in the presence of isopropylthiogalactoside (IPTG). Because LacI did not interact with the LacO array in the presence of IPTG, the LacI fusion proteins did not localize to the LacO locus. To localize the fusion proteins to the LacO locus, we washed off the IPTG and activated Cre recombinase by adding 4-hydroxytamoxifen (OHT) to remove the native centromere (Fig. 1B,C). We then isolated the surviving colonies after 10–14 days of incubation. When we used LacI-fused EGFP (control), we only isolated approximately three colonies per 10^5 cells, values that are similar to those of our previous studies (Hori et al., 2013; Shang et al., 2013). A previous analysis of surviving clones demonstrated that chromosome Z lacking the centromere fused to another chromosome or acquired a neocentromere at a low frequency to prevent chromosome loss (Shang et al., 2013). Importantly, the survival rate was ten to 50 times higher in cells expressing LacI fusions with the HJURP N-terminus (aa 1–400), Knl2, CENP-C, CENP-C C-terminus (aa 601–864) or CENP-I (Fig. 1D). Because the native centromere of chromosome Z was removed from these cells, a new centromere was expected to form at the LacO locus. CENP-A was only detected near a native centromeric position in control cells expressing LacI-fused EGFP (Figs S1A and S2A,B), whereas in cells expressing either the HJURP N-terminus (aa 1–400), Knl2, CENP-C, CENP-C C-terminus (aa 601–864) or CENP-I, CENP-A was detected at the LacO locus after removal of a native centromere (Fig. 1E). Furthermore, a CCAN protein (CENP-T) and a KMN protein (Dsn1) were detected at the LacO locus tethered by the LacI-fused HJURP N-terminus (aa 1–400), Knl2, CENP-C, CENP-C C-terminus (aa 601–864) or CENP-I, indicating that a full kinetochore was formed at the LacO locus by tethering of the HJURP N-terminus (aa 1–400), Knl2, CENP-C, CENP-C C-terminus (aa 601–864) or CENP-I. Cells containing these artificial kinetochores at the LacO locus proliferated normally in the presence of IPTG (Fig. 1F). This suggests that the artificial kinetochore functions similar to the native kinetochore and recruits CENP-A. In contrast, cells containing an artificial kinetochore tethered by the CENP-T N-terminus (aa 1-530) died after IPTG addition (Fig. 1G), likely because this artificial kinetochore does not have CENP-A (Hori et al., 2013). Once CENP-A was incorporated at the locus, further tethering of target proteins was not needed, because each artificial kinetochore functions even in the presence of IPTG.

CENP-A incorporation occurs at the LacO locus tethered by the HJURP N-terminus, Knl2, CENP-C, CENP-C C-terminus or CENP-I

Stable incorporation of CENP-A into the LacO locus resulted in artificial kinetochore formation. Thus, to understand the mechanisms of artificial kinetochore formation, analyzing how CENP-A is incorporated into the LacO locus is critical. To directly observe CENP-A incorporation at the LacO locus by tethering of the HJURP N-terminus, Knl2, CENP-C, the CENP-C C-terminus and CENP-I, we introduced mScarlet-fused CENP-A cDNA into the β-actin (*ACTB*) locus (Fig. S1A). We note that CENP-A under control of the β-actin promoter was expressed approximately three times more than endogenous CENP-A (Fig. S1G,H). Next, mScarlet–CENP-A was stably expressed in each cell line and mScarlet intensities at the LacO locus were evaluated 1, 2 and 3 days after IPTG washout (Fig. 2A–C). We also measured the EGFP signals of the LacI-fused proteins at the LacO locus (Fig. 2B,D). LacI-fused centromeric proteins, except HJURP, were clearly visible from day 1 after IPTG washout, similar to EGFP–LacI (control). In addition to the LacO locus, the EGFP signals of centromeric proteins were detected at the native centromere on chromosome Z (Fig. 2B). CENP-A signals were not clear at the LacO locus on day 1 following tethering of Knl2, CENP-C, CENP-C C-terminus and CENP-I. However, CENP-A signals were visible by day 3 following tethering of Knl2, CENP-C, CENP-C C-terminus and CENP-I to the LacO locus (Fig. 2B,C,E), whereas CENP-A signals were not observed at the LacO locus by tethering of EGFP–LacI (control). We note that although CENP-A signals at the LacO locus observed at 3 days after tethering of these proteins were similar to those at endogenous centromeres, the efficiency of functional kinetochore formation at the LacO locus was still $2–15\times10^{-4}$ (Fig. 1D), suggesting that additional mechanisms for CENP-A incorporation are required for the establishment of functional kinetochores. Nevertheless, we would like to emphasize that tethering of Knl2, CENP-C, CENP-C C-terminus and CENP-I to the LacO locus significantly increased efficiencies of kinetochore formation (10–50 times). For HJURP tethering, CENP-A was visible from day 1, and its levels were more than ten times higher than those for tethering of Knl2, CENP-C, CENP-C C-terminus or CENP-I (Fig. 2B,C). This could be attributed to the direct binding of HJURP to CENP-A. Furthermore, as CENP-A levels might have been saturated at the LacO locus and excess CENP-A is toxic, HJURP might have been maintained at lower levels, indicating why it was difficult to visualize EGFP–HJURP (aa 1–400)–LacI at the LacO locus (Fig. 2B,D). In addition, HJURP localizes to centromeres at G1 phase (Perpelescu et al., 2015), and it is not easy to detect its localization at mitotic chromosomes. However, we note that EGFP–HJURP (aa 1–400) was approximately 1.8 times overexpressed compared with endogenous HJURP levels, based on an immunoblot analysis (Fig. S3A). Furthermore, EGFP–HJURP (aa 1–400) localized at endogenous centromeres in addition to the LacO locus (Fig. S3B). This explains why CENP-A incorporation was also increased at endogenous centromeres (Fig. 2B). Although CENP-A levels were high by HJURP tethering, tethering of Knl2, CENP-C, CENP-C C-terminus and CENP-I induced CENP-A incorporation at the LacO locus by day 3 (Fig. 2C), leading to artificial kinetochore formation at the LacO locus.

Journal of Cell Science (2024) 137, jcs261639. doi:10.1242/jcs.261639

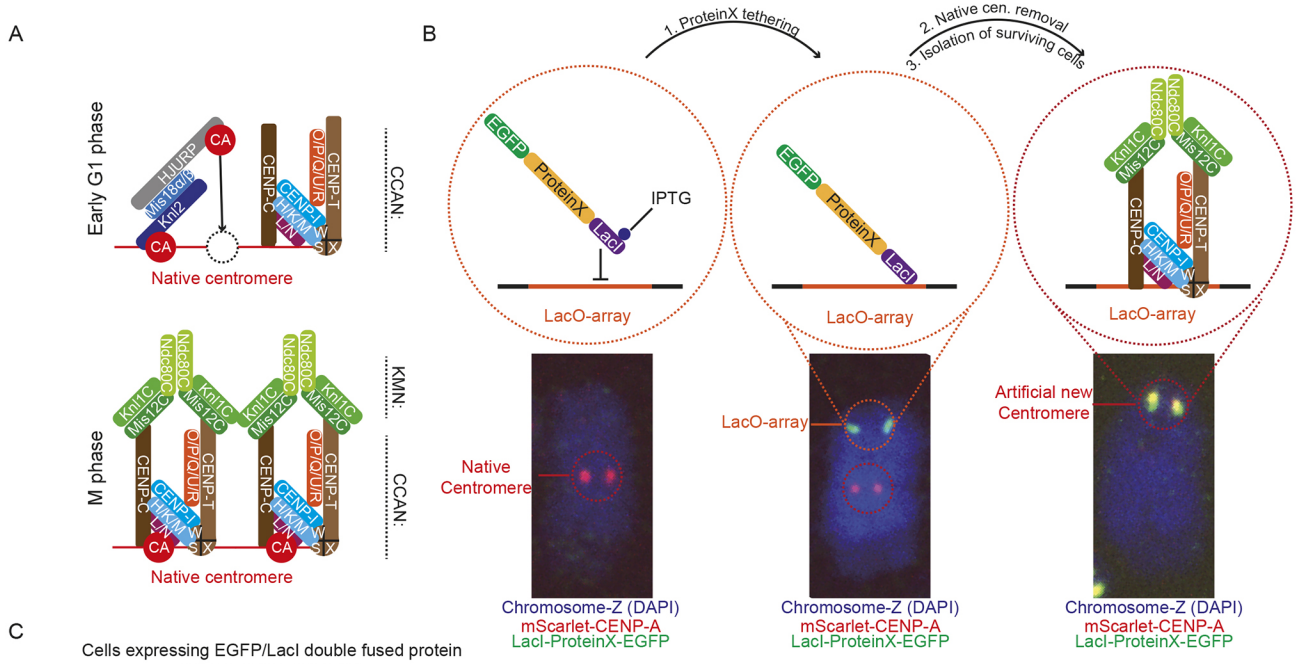

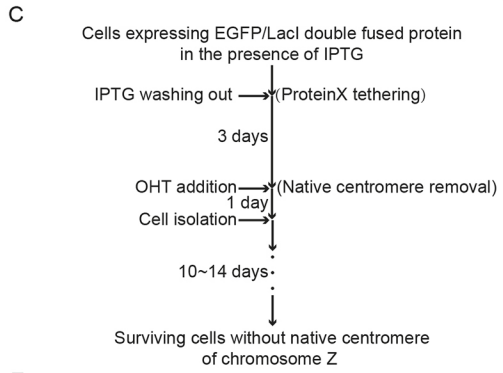

D

Tethered Protein	Number of surviving cells (/10^5 cells)
HJURP(1-400)	25±5
Knl2	25±9
CENP-I	46±21
CENP-C	71±23
CENP-C(601-864)	147±33
None	3±1

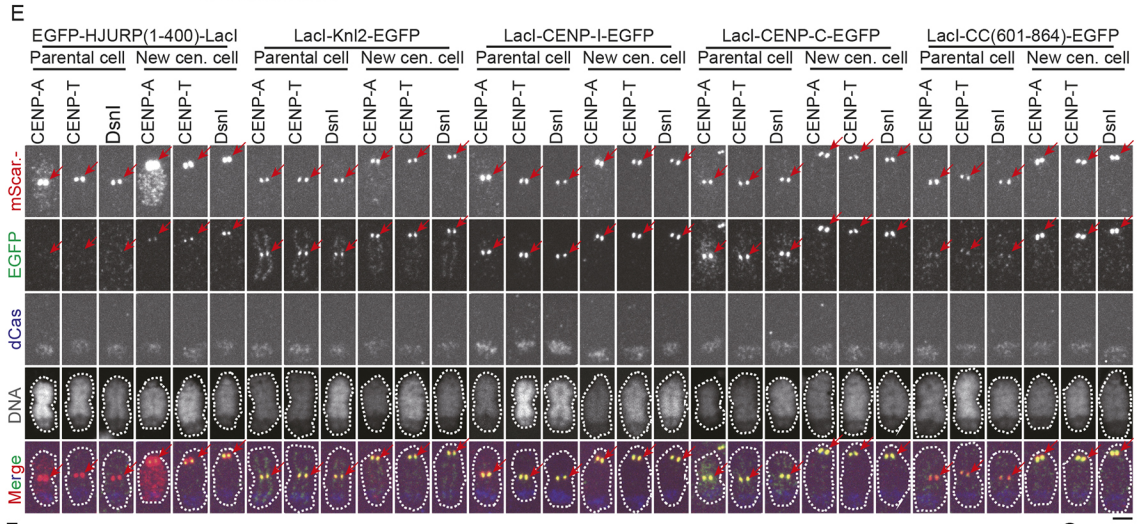

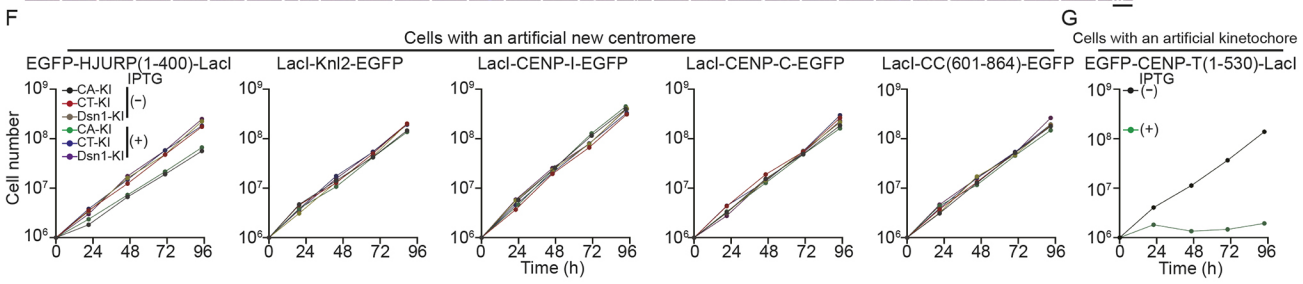

Fig. 1. See next page for legend.

Journal of Cell Science (2024) 137, jcs261639. doi:10.1242/jcs.261639

Fig. 1. Ectopic localization of inner kinetochore proteins induces efficient formation of artificial new kinetochores at a non-centromeric locus. (A) Centromere components used in this study. Knl2 and Mis18α/β form a complex (Mis18 complex) and associate with centromeric chromatin. HJURP associated with CENP-A (CA) recognizes the Mis18 complex and new CENP-A is incorporated into centromeres during the G1 phase. Constitutive centromere-associated network (CCAN) components including CENP-C or CENP-I associate with centromeric chromatin. The microtubule-bunding KMN network is recruited onto CCAN to form a functional kinetochore in mitosis. (B) An experimental design to generate a new kinetochore at a non-centromeric locus using an inserted LacO array on chicken chromosome Z following removal of the native centromere. Cells were maintained in the presence of IPTG to inhibit the interaction between LacO and the LacI fusion protein (X). Upon IPTG removal, the LacI-fused protein X was allowed to bind to the LacO array and initiated the incorporation of CENP-A. Finally, Cre recombinase was activated to delete the native centromere of chromosome Z, and the artificial kinetochore was confirmed to be functional. Once CENP-A was incorporated, the artificial kinetochore became functional, even in the presence of IPTG. (C) The experimental time course for B. The chicken DT40 cell line expressing the EGFP/LacI-fused protein X was cultured in the presence of IPTG, and the assay was performed after IPTG removal (day 0). Following a 3-day incubation, 4-hydroxytamoxifen (OHT) was added to activate Cre recombinase. After an additional 1-day incubation, the cells were plated and grown for 10–14 days to isolate surviving cells. (D) The number of surviving colonies per 10^5 cells, when EGFP/LacI double-fused HJURP (aa 1–400), Knl2, CENP-I, CENP-C or CENP-C (aa 601–864) were localized to the LacO locus after removing the native centromere on chromosome Z. Each assay was conducted twice, and the results depict the mean±s.d. (E) Visualization of chromosome Z in cells expressing EGFP/LacI double-fused HJURP (aa 1–400), Knl2, CENP-I, CENP-C or CENP-C (aa 601–864) before and after the new kinetochore formation assay. mScarlet-tagged CENP-A, CENP-T and Dsn1 were visualized. A Halo-tagged dCas protein along with sgRNA was used to label the specific satellite sequence at the end of the q-arm on chromosome Z. New kinetochores were formed at the LacO locus, and the inner (CENP-T) and outer (Dsn1) kinetochore proteins were localized at the new kinetochore. Merged images of mScarlet-tagged proteins, EGFP/LacI double-fused proteins and Halo-tagged dCas, with the outline of chromosome Z are shown at the bottom. Centromeres are indicated by red arrows. Scale bar: 2.5 µm. (F) The proliferation of cells with an artificial new centromere formed on chromosome Z is shown in the absence or presence of IPTG. Data for cell lines with tethering of EGFP/LacI double-fused HJURP (aa 1–400), Knl2, CENP-I, CENP-C or CENP-C (aa 601–864) to the LacO locus are shown. Each kind of tethered cell line expressed mScarlet-fused CENP-A (CA-KI), CENP-T (CT-KI) or Dsn1 (Dsn1-KI) separately. (G) The proliferation of cells with an artificial new kinetochore tethered by the CENP-T N-terminus (aa 1–530) is shown in the absence or presence of IPTG.

Tethering of the CENP-C C-terminus or CENP-I induces CENP-A incorporation in the absence of Knl2

HJURP is a CENP-A-specific chaperone and Knl2 is a member of the Mis18 complex, which recognizes HJURP for new CENP-A incorporation. Therefore, we can explain how the tethering of HJURP or Knl2 induces CENP-A incorporation. However, the mechanism by which tethering of the CENP-C C-terminus or CENP-I induces CENP-A incorporation remains unclear. To examine how the CENP-C C-terminus or CENP-I induces CENP-A incorporation, we combined an AID-based protein knockout system with a tethering assay (Fig. 3A, Figs S1A and S4A). Upon HJURP depletion in cells (Fig. S1B), no tethering-induced CENP-A incorporation was observed at the LacO locus (Fig. 3B,C), indicating that HJURP is the most critical component for CENP-A incorporation. We note that HJURP was overexpressed in our AID–HJURP cells before knockout (Fig. S1B), although this overexpressed HJURP was rapidly degraded after auxin addition. In addition to the LacO locus, CENP-A levels at endogenous centromeres were also reduced in HJURP-knockout cells (approximately 25% reduction after 1 day, Fig. S3C). As it takes approximately 8–10 h to complete one cell cycle in DT40 cells, two to three cell cycles are completed in 1 day. If CENP-A incorporation was stopped, the existence of CENP-A would be reduced to half in each cell cycle. Therefore, we interpret that the reduction of CENP-A at endogenous centromeres is due to dilution of CENP-A after each cell-cycle progression. We further investigated the effects of Knl2 depletion (Fig. S1C). Because HJURP recognizes the Mis18 complex, including Knl2, we expected that CENP-C or CENP-I tethering would not induce CENP-A incorporation in the absence of Knl2. However, tethering of the CENP-C C-terminus or CENP-I to the LacO locus induced CENP-A incorporation even in the absence of Knl2 (Fig. 3D,E; Fig. S4B,C). We also found that tethering of the CENP-C C-terminus to the LacO locus induced CENP-A incorporation in Mis18α-knockout cells (Fig. 3F,G; Figs S1D, S4D and S4E). These results suggest that the CENP-C C-terminus induced CENP-A incorporation in the absence of the Mis18 complex and we further examined a mechanism for how CENP-A is incorporated at the LacO locus by tethering of CENP-I or CENP-C C-terminus in the absence of Knl2.

To further investigate CENP-A incorporation mechanisms by protein tethering to the LacO locus, we tested CENP-C-depleted cells (Fig. S1E). We examined the tethering of Knl2 or CENP-I into the LacO locus in CENP-C-depleted cells. Knl2 tethering induced CENP-A incorporation in the absence of CENP-C (Fig. 3H,I; Fig. S4F,G), suggesting that once Knl2 was tethered to the LacO locus, CENP-A was incorporated via Mis18 complex formation in the absence of CENP-C. In contrast, CENP-I tethering did not induce CENP-A incorporation into the LacO locus in CENP-C-depleted cells (Fig. 3H,I; Fig. S4F,G). We also note that endogenous CENP-A levels were not dramatically changed in Knl2- or CENP-C-knockout cells unlike in HJURP-knockout cells (Fig. 3B,D,H), and we discuss this point in the Discussion section.

Because CENP-I is known to interact with CENP-C, we examined whether tethering of the CENP-C C-terminus induces CENP-A incorporation into the LacO locus in the absence of CENP-I. CENP-I depletion is known to cause a strong mitotic arrest (Nishihashi et al., 2002) and observing CENP-A incorporation is difficult because CENP-A deposition occurs in the G1 phase. To solve this problem, we added reversine, an inhibitor of the spindle checkpoint (Santaguida et al., 2010), to CENP-I-knockout cells treated with nocodazole with expression of HJURP (Fig. 3J). We note that HJURP expression supported steady CENP-A incorporation in Knl2-, Mis18α- or CENP-C-knockout cells (Fig. S4); therefore, we evaluated CENP-A incorporation in CENP-I-knockout cells expressing HJURP and detected CENP-A incorporation by tethering of the CENP-C C-terminus in CENP-I-knockout cells (Fig. 3K,L). We also confirmed CENP-A incorporation by CENP-C C-terminus tethering in Knl2-, Mis18 α- and CENP-C-knockout cells using the reversine method (Fig. S5A,B).

The results of these analyses are summarized in Fig. 3M. In the absence of HJURP, tethering of any proteins did not induce CENP-A incorporation into the LacO locus. Interestingly, tethering of the CENP-C C-terminus and CENP-I induced CENP-A incorporation at the LacO locus in the absence of Knl2 (Fig. 3D,E; Fig. S4B,C), and CENP-C C-terminus tethering induced CENP-A incorporation in the Mis18α-knockout cells (Fig. 3F,G; Fig. S4D,E), suggesting that the CENP-C C-terminus or CENP-I induce CENP-A incorporation at the LacO locus independently of the Mis18 complex. Although both the CENP-C C-terminus and CENP-I induced CENP-A incorporation, the CENP-C C-terminus induced CENP-A incorporation in the absence of CENP-I (Fig. 3K,L), but

Journal of Cell Science (2024) 137, jcs261639. doi:10.1242/jcs.261639

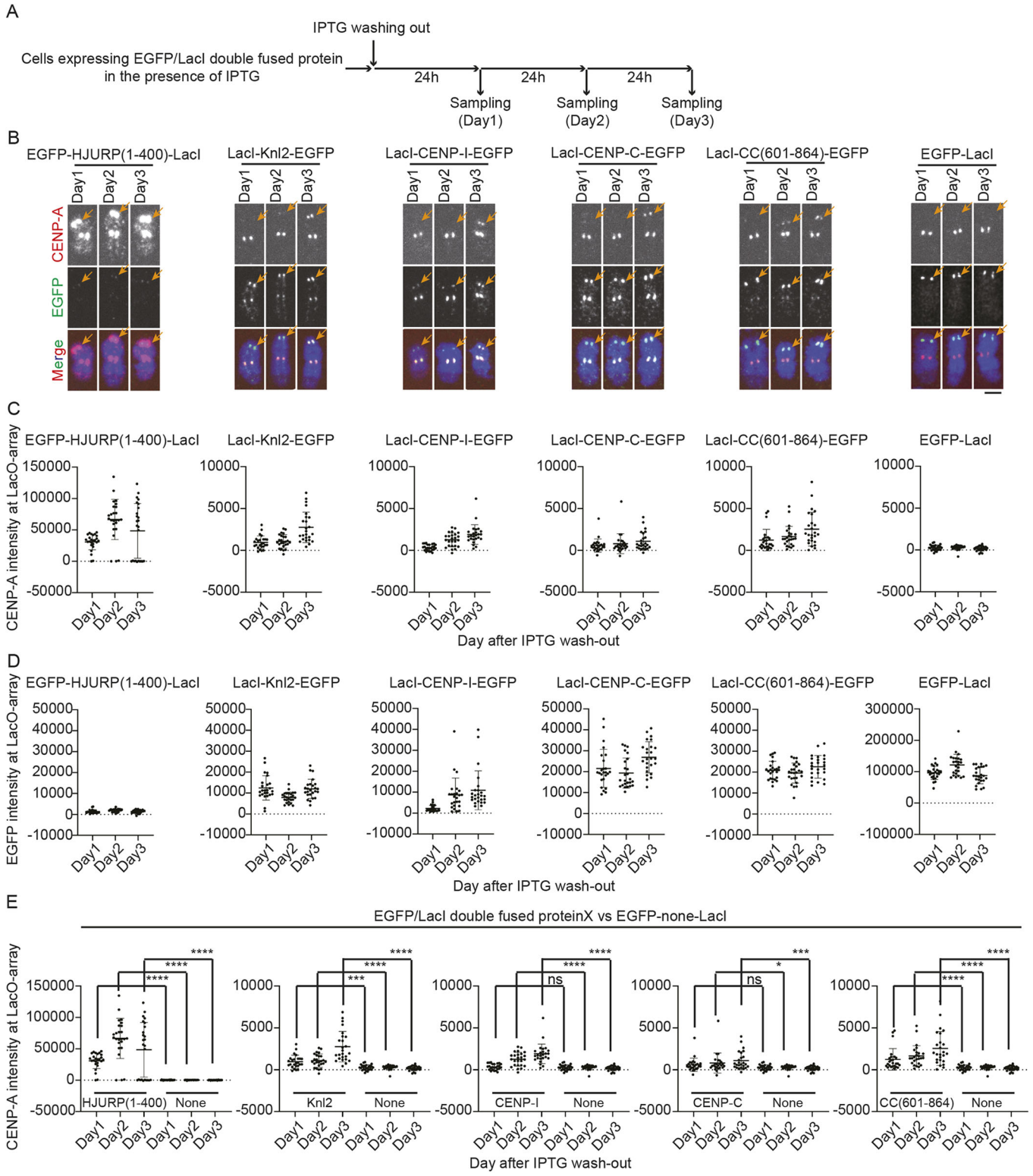

Fig. 2. CENP-A incorporation occurs at the LacO locus after the tethering of HJURP, Knl2, CENP-I, CENP-C or CENP-C C-terminus. (A) Experimental scheme for visualizing centromeric proteins at the LacO locus. The chicken DT40 cells expressing the EGFP/LacI double-fused protein X were cultured in the presence of IPTG, and the assay was initiated after IPTG removal (day 0). Chromosome spreads were prepared for 3 days to observe CENP-A and other centromeric proteins at the LacO locus each day. (B) Visualization of mScarlet-tagged CENP-A and EGFP/LacI double-fused HJURP (aa 1–400), KNL2, CENP-I, CENP-C or CENP-C C-terminus or empty target protein at the LacO locus on chromosome Z on days 1, 2 and 3 as shown in A. Merged images of mScarlet-tagged CENP-A, EGFP/LacI double-fused proteins and DAPI-stained chromosome Z are shown on the bottom. The LacO locus is indicated by orange arrows. Scale bar: 2.5 µm. (C,D) The intensities (arbitrary units) of the mScarlet-tagged CENP-A (C) and the EGFP/LacI double-fused proteins (D) at the LacO locus in each cell line (B) are shown. Bars show the mean±s.d. of the intensity values. *n*=25. The CENP-A dataset for cells with LacI–CENP-C (aa 601–864)–EGFP (C) is identical to that shown for CC (aa 601–864) in Fig. 6E. (E) Significance of CENP-A incorporation by protein tethering shown in B,C. *n*=25. In C–E, bars show the mean±s.d. ns, not significant, $P>0.05$; *$P\leq0.05$; ***$P\leq0.001$; ****$P<0.0001$; unpaired two-tailed *t*-test.

Journal of Cell Science (2024) 137, jcs261639. doi:10.1242/jcs.261639

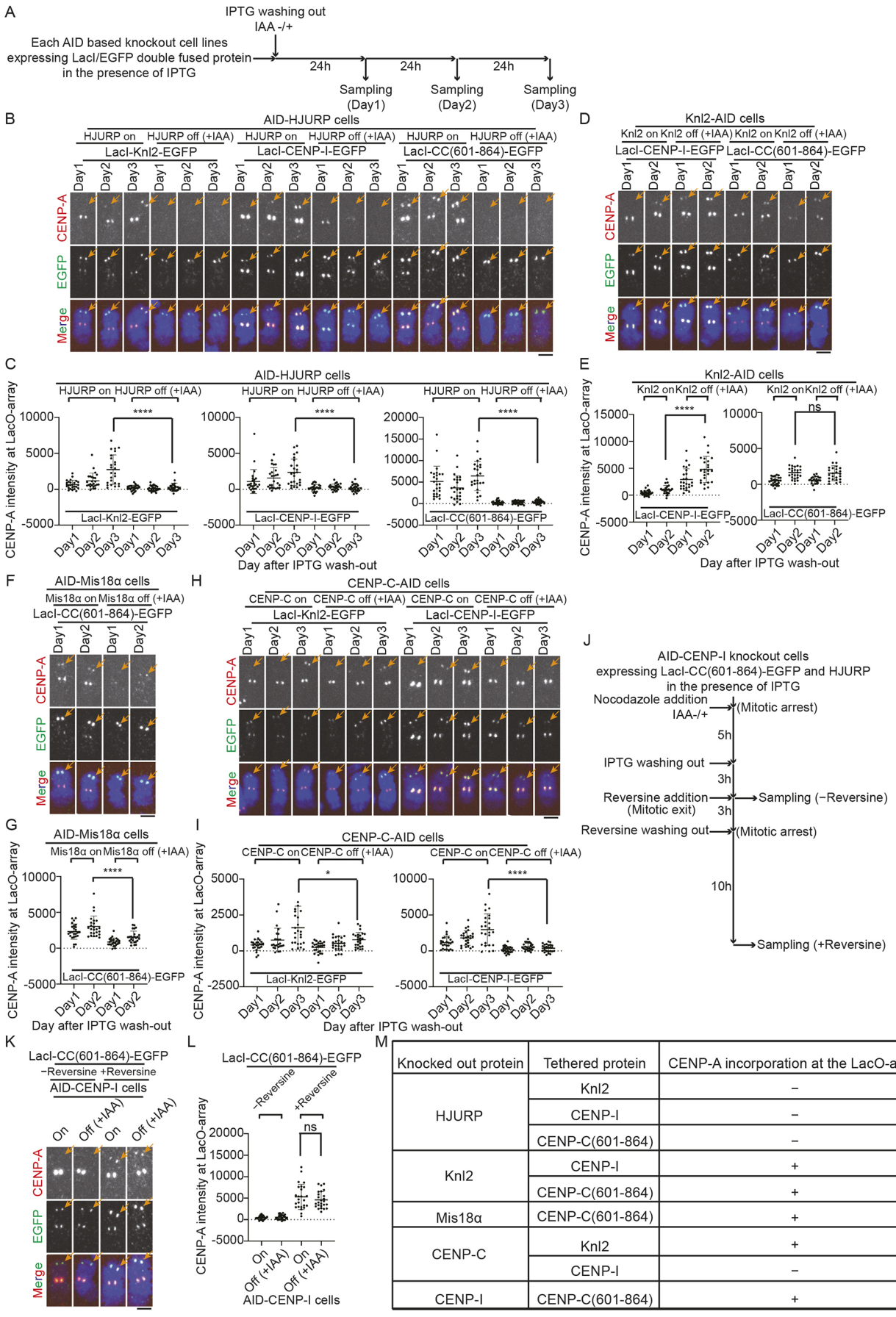

M

Knocked out protein	Tethered protein	CENP-A incorporation at the LacO-array
HJURP	Knl2	–
	CENP-I	–
	CENP-C(601-864)	–
Knl2	CENP-I	+
	CENP-C(601-864)	+
Mis18α	CENP-C(601-864)	+
CENP-C	Knl2	+
	CENP-I	–
CENP-I	CENP-C(601-864)	+

Fig. 3. See next page for legend.

Journal of Cell Science (2024) 137, jcs261639. doi:10.1242/jcs.261639

Fig. 3. Tethering of CENP-I or the CENP-C C-terminus induces CENP-A incorporation in the absence of Knl2. (A) Experimental scheme for visualizing CENP-A and other centromeric proteins at the LacO locus in auxin-inducible degron (AID)-based knockout cells. Cells were cultured in the presence of IPTG, and the assay commenced after IPTG removal (day 0) in the absence or presence of indole-3-acetic acid (IAA). Chromosome spreads were prepared for 3 days (2 days for Knl2- and Mis18α-knockout cells due to cell death) to observe CENP-A and other centromeric proteins at the LacO locus each day. (B) Visualization of mScarlet-tagged CENP-A and LacI/EGFP double-fused Knl2, CENP-I and CENP-C (aa 601–864) at the LacO locus on chromosome Z on days 1, 2 and 3 (as shown in A) in AID–HJURP cells in the absence (HJURP on) or presence (HJURP off) of IAA. (C) The intensities (arbitrary units) of mScarlet-tagged CENP-A at the LacO locus in AID–HJURP cells in the absence (HJURP on) or presence (HJURP off) of IAA are shown. (D) Visualization of mScarlet-tagged CENP-A and LacI/EGFP double-fused CENP-I and CENP-C (aa 601–864) at the LacO locus on chromosome Z on days 1 and 2 in Knl2–AID cells in the absence (Knl2 on) or presence (Knl2 off) of IAA. (E) The intensities (arbitrary units) of mScarlet-tagged CENP-A at the LacO locus in Knl2–AID cells in the absence (Knl2 on) or presence (Knl2 off) of IAA are shown. (F) Visualization of mScarlet-tagged CENP-A and LacI/EGFP double-fused CENP-C (aa 601–864) at the LacO locus on chromosome Z at days 1 and 2 in AID–Mis18α cells in the absence (Mis18α on) or presence (Mis18α off) of IAA. (G) The intensities (arbitrary units) of mScarlet-tagged CENP-A at the LacO locus is shown in AID–Mis18α cells in the absence (Mis18α on) or presence (Mis18α off) of IAA. (H) Visualization of mScarlet-tagged CENP-A and LacI/EGFP double-fused Knl2 and CENP-I at the LacO locus on chromosome Z at days 1, 2 and 3 in CENP-C–AID cells in the absence (CENP-C on) or presence (CENP-C off) of IAA. (I) The intensities (arbitrary units) of mScarlet-tagged CENP-A at the LacO locus is shown in CENP-C–AID cells in the absence (CENP-C on) or presence (CENP-C off) of IAA. The data set for CENP-C–AID cells with LacI–CENP-I–EGFP (right-hand graph) is identical to that shown for no Halo–CENP-C expression (None) in Fig. 5C. (J) Experimental scheme to visualize CENP-A and other centromeric proteins at the LacO locus in AID–CENP-I cells expressing LacI/EGFP double-fused CENP-C (aa 601–864). These cells were cultured in the presence of IPTG, and the assay commenced with the addition of nocodazole in either the absence or presence of IAA. After 5 h of incubation, IPTG was washed out. Following an additional 3 h of incubation, chromosome spreads were prepared using some of the described cells (−reversine). The remaining cells were treated with reversine for 3 h, followed by a washout of reversine. After a subsequent 10 h incubation, chromosome spreads were prepared (+reversine). (K) Visualization of mScarlet-tagged CENP-A and LacI/EGFP double-fused CENP-C (aa 601–864) at the LacO locus in AID-based CENP-I-knockout cells. Visualization was performed before and after adding reversine, in the absence or presence of IAA according to H. (L) The intensities (arbitrary units) of mScarlet-tagged CENP-A at the LacO locus in AID–CENP-I cells in the absence (CENP-I on) or presence (CENP-I off) of IAA is shown. In B,D, F,H,K, merged images of mScarlet-tagged CENP-A, LacI/EGFP double-fused proteins and DAPI-stained chromosome Z are shown on the bottom. The LacO locus is indicated by orange arrows. All scale bars: 2.5 µm. In C,E, G,I,L, bars show the mean±s.d. of the intensity values (ns, not significant, $P>0.05$; *$P\leq0.05$; ****$P<0.0001$; unpaired two-tailed *t*-test). (M) Summary of requirements for CENP-A incorporation at the LacO locus induced by Knl2, CENP-I or CENP-C C-terminus tethering.

CENP-I did not do so in the absence of CENP-C (Fig. 3H,I; Fig. S4F,G), suggesting that CENP-I-based CENP-A incorporation occurs via CENP-C.

CENP-A recruitment by CENP-I tethering requires proper CCAN formation

Whereas CENP-I tethering induced CENP-A incorporation, it is unclear whether CENP-I needs to form a complex with other CCAN proteins for the induction of CENP-A incorporation. Recent structural analyses on the CCAN complex using cryo-electron microscopy have revealed a structural model of the human CCAN complex (Pesenti et al., 2022; Tian et al., 2022; Yatskevich et al., 2022). Based on these structural models, we predicted a homology model of the chicken CENP-H–CENP-I–CENP-K–CENP-M (hereafter CENP-H/I/K/M) complex (Fig. 4A). In this homology model, V136, V139, L175 and I178 of chicken CENP-I appeared to bind W212 of chicken CENP-H (Fig. 4A,B). To evaluate these four residues in CENP-I, we generated the cDNA of mutant CENP-I (CENP-I^{4A}), in which V136, V139, L175 and I178 were replaced with alanine, and expressed this mutant CENP-I^{4A} in tetracycline (Tet)-responsive CENP-I conditional knockout (cKO) cells (Nishihashi et al., 2002). In the cKO line, CENP-I expression was turned off upon Tet addition, and the cells died ∼96 h after Tet addition (Fig. 4C). When wild-type CENP-I (CENP-I^{WT}–EGFP) was expressed in CENP-I cKO cells, cell death was suppressed, even after Tet addition (Fig. 4C; Fig. S6A). However, expression of CENP-I^{4A} (CENP-I^{4A}–EGFP) did not suppress cell death in CENP-I cKO cells after Tet addition (Fig. 4C; Fig. S6A), suggesting that CENP-I^{4A} is not functional. To support this result, we examined CENP-H/I/K/M complex formation by co-immunoprecipitation. We prepared cell lines expressing EGFP-fused CENP-I^{WT} or CENP-I^{4A}, and immunoprecipitated the cell-lysate using an anti-GFP antibody. CENP-I was recovered from both cell lines and CENP-C, CENP-H, CENP-K and CENP-M were detected in cells expressing CENP-I^{WT}–EGFP. However, these CENP proteins were not detected in cells expressing CENP-I^{4A}–EGFP (Fig. 4D). These results suggest that CENP-I^{4A} does not form the CENP-H/I/K/M complex and is therefore not functional in this context. Consistent with these immunoprecipitation results, CENP-I^{4A}–EGFP did not localize to kinetochores (Fig. 4E).

We then tested whether CENP-I^{4A} could induce CENP-A incorporation at the LacO locus without the CENP-H/I/K/M complex formation. Whereas CENP-I^{WT} tethering induced CENP-A incorporation at the LacO locus, CENP-I^{4A} did not (Fig. 4F,G). Although we confirmed localization of LacI–CENP-I^{4A}–EGFP at the LacO locus (Fig. 4F,H), CENP-C was not detected at the LacO locus following CENP-I^{4A} tethering (Fig. 4F,I). These results suggest that CENP-I alone may not have the ability to induce CENP-A incorporation because CENP-H/I/K/M complex formation is required for CENP-C recruitment, which might be essential for inducing CENP-A incorporation at the LacO locus. We should also note that whereas CENP-I^{4A} localized at the LacO locus, the levels were low compared with those of CENP-I^{WT} (Fig. 4H). Therefore, weak tethering of CENP-I^{4A} might be a reason why CENP-A induction did not occur.

The CENP-C–CENP-I interaction is essential for CENP-A incorporation by CENP-I tethering at the LacO locus

As described above, CENP-I tethering did not induce CENP-A incorporation at the LacO locus in the absence of CENP-C (Fig. 3H,I; Fig. S4F,G). Furthermore, the CENP-I^{4A} mutant, which did not form the CENP-H/I/K/M complex, did not recruit CENP-C and not induce CENP-A incorporation at the LacO locus (Fig. 4F–I). These results suggest that CENP-I tethering requires CENP-C for CENP-A incorporation at the LacO locus, and that the CENP-C–CENP-I interaction is essential for this process. Previous studies have clearly demonstrated that the middle conserved region of CENP-C [aa 166–324 region of chicken CENP-C, CCAN-binding domain (CBD)] interacts with the CENP-H/I/K/M complex (Basilico et al., 2014; Hara et al., 2023; Klare et al., 2015; McKinley et al., 2015; Nagpal et al., 2015). We then prepared CENP-C cKO cell lines expressing a CENP-C mutant lacking aa 166–324 (CENP-C$^{\Delta CBD}$), which is a critical region for binding to the CENP-H/I/K/M complex (Fig. 5A; Fig. S6B), and used this line for the CENP-I tethering assay. As expected, CENP-C$^{\Delta CBD}$ did not localize to the LacO locus by CENP-I tethering

Journal of Cell Science (2024) 137, jcs261639. doi:10.1242/jcs.261639

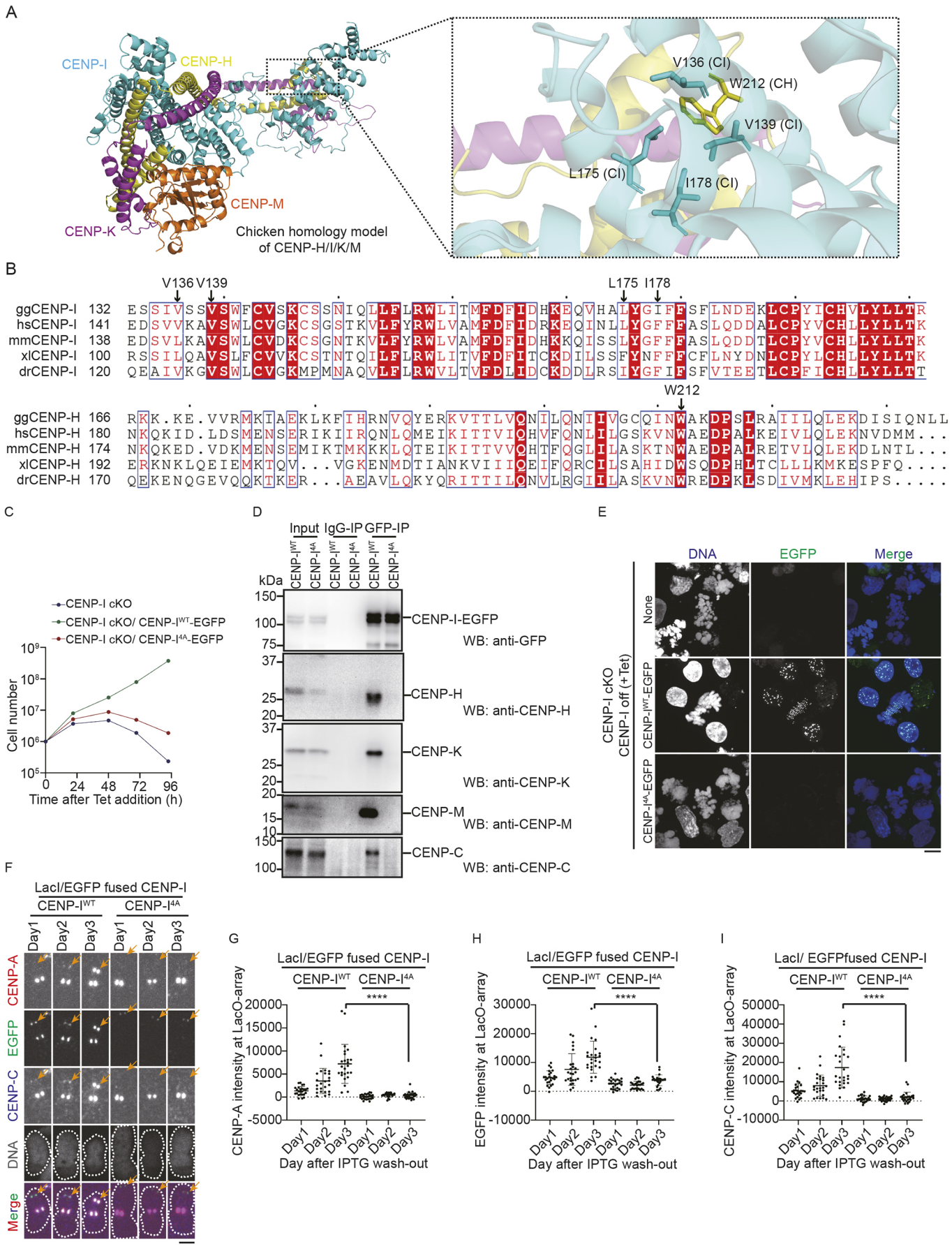

Fig. 4. See next page for legend.

Journal of Cell Science

Fig. 4. CCAN formation is required for CENP-A incorporation at the LacO locus by tethering of CENP-I. (A) The homology model of chicken CENP-H/I/K/M. The magnified view shows a hydrophobic interaction site between CENP-H (CH) and CENP-I (CI) in the CENP-I N-terminal heat repeat, with critical residues presented for clarity. (B) Alignment of CENP-I N-terminal and CENP-H C-terminal sequences in various species. These regions are expected to be involved in the hydrophobic interactions between CENP-H and CENP-I. The predicted critical residues involved in this interaction are shown. (C) Growth curves of cKO CENP-I cells expressing EGFP-fused ggCENP-I^{WT} or CENP-I^{4A} at the indicated time points after Tet addition. (D) Immunoprecipitation (IP) was performed using an anti-GFP antibody in cKO CENP-I cells expressing CENP-I^{WT}–EGFP or CENP-I^{4A}–EGFP in the presence of Tet for 12 h. The immunoprecipitated samples were detected using antibodies specific to CENP-H, CENP-K, CENP-M and CENP-C by western blotting (WB). *n*=2. (E) Localization of EGFP-fused ggCENP-I^{WT} or CENP-I^{4A} in cKO-CENP-I cells in the presence of Tet. Scale bar: 10 µm. (F) Visualization of mScarlet-tagged CENP-A, LacI/EGFP double-fused CENP-I (CENP-I^{WT} or CENP-I^{4A}) and Halo-tagged CENP-C at the LacO locus on chromosome Z on days 1, 2 and 3 after IPTG removal. Merged images of mScarlet-tagged CENP-A, LacI/EGFP double-fused CENP-I (WT or 4A) and Halo-tagged CENP-C with the outline of chromosome Z are shown on the bottom. The LacO locus is indicated by an orange arrow. Scale bar: 2.5 µm. (G–I) The intensities (arbitrary units) of mScarlet-tagged CENP-A (G), LacI/EGFP double-fused proteins (H) and Halo-tagged CENP-C (I) at the LacO locus in cells expressing LacI/EGFP double fused CENP-I^{WT} or CENP-I^{4A} is shown. Bars show the mean±s.d. of the intensity values (*n*=25). ****P<0.0001; unpaired two-tailed *t*-test.

(Fig. 5B,E). Consistent with the results shown in Fig. 3H,I and Fig. S4F,G, in CENP-C-knockout cells, CENP-A was not detected at the LacO locus after CENP-I tethering on day 3 (Fig. 5B). However, the expression of Halo-tagged CENP-C^{WT} rescued CENP-A incorporation at the LacO locus via CENP-I tethering. In contrast, the expression of Halo-tagged CENP-C$^{\Delta CBD}$ did not rescue CENP-A incorporation at the LacO locus by CENP-I tethering (Fig. 5B–E), suggesting that CENP-A incorporation at the LacO locus by CENP-I tethering requires the interaction of CENP-C with the CENP-H/I/K/M complex.

CENP-C binds to HJURP to induce CENP-A incorporation at the LacO locus

CENP-C C-terminus tethering induced CENP-A incorporation at the LacO locus even in the absence of CENP-I, Mis18α or Knl2 (Fig. 3; Figs S4 and S5). In addition, CENP-A incorporation at the LacO locus by CENP-I tethering required CENP-C to interact with the CENP-H/I/K/M complex (Fig. 5). These results suggest that CENP-C directly binds to HJURP to induce CENP-A incorporation at the LacO locus, which might be independent of the Mis18 complex–HJURP pathway. To test this hypothesis, we examined whether CENP-C co-precipitates with HJURP. We transiently expressed FLAG-tagged HJURP (either FL, aa 1–254 or aa 255–772) with EGFP-tagged FL CENP-C or various versions of the CENP-C C-terminus (Fig. 6A) and performed immunoprecipitation with an anti-GFP antibody. We detected FLAG–HJURP using immunoblot analysis of the immunoprecipitates with an anti-GFP antibody in cells expressing EGFP–CENP-C and FLAG–HJURP (Fig. 6B). We found that the N-terminal region of HJURP (aa 1–254) co-precipitated with CENP-C but not with the C-terminal region of HJURP (Fig. 6B). We further examined the region of CENP-C that co-precipitated with HJURP. We detected HJURP, when CENP-C (aa 601–864) was precipitated. However, we did not detect HJURP in anti-GFP precipitates expressing shorter EGFP–CENP-C C-terminal fragments (aa 721–864 or aa 601–720), suggesting that these CENP-C regions are required but not sufficient for the CENP-C–HJURP interaction. We also tested the importance of the CENP-C dimer interface (Y799 and H843) for HJURP interaction by replacing these residues with alanine. This mutant CENP-C C-terminus [aa 601–864, Y799A, H843A; CENP-C(601–864)^{2A}] co-precipitated with FLAG–HJURP (Fig. 6C). This result in chicken cells is slightly different from that in *Xenopus* cells (Flores Servin et al., 2023).

We examined whether these CENP-C C-terminal fragments induced incorporation of CENP-A at the LacO locus. Although tethering of wild-type CENP-C (aa 601–864) induced CENP-A incorporation at the LacO locus, tethering of CENP-C mutants that did not co-precipitate with HJURP did not (Fig. 6D,E). Tethering of CENP-C(601–864)^{2A} induced significant CENP-A incorporation into clone #2 cells; however, the efficiency was not the same as that of wild-type CENP-C (Fig. 6D,E). We note that significant CENP-A incorporation did not occur in clone #1. As CENP-C(601–864)^{2A} co-precipitates with HJURP, CENP-C(601–864)^{2A} tethering can be assumed to induce CENP-A incorporation at the LacO locus. However, CENP-C(Y799A, H843A) might be unstable compared to wild-type CENP-C.

Finally, we examined HJURP localization at the LacO locus by tethering the CENP-C C-terminal fragment. HJURP localization is strictly regulated at native centromeres, and it localizes at centromeres only during the G1 phase and disappears from centromeres in the S/G2/M phases. Consistent with native HJURP localization, the HJURP signal was detected at the LacO locus in interphase cells but not in mitotic cells by tethering CENP-C (aa 601–864) (Fig. 6F). As CENP-C does not require Knl2 for CENP-C–HJURP interaction in chicken cells (Fig. 6B,C); CENP-C (aa 601–864) directly recruits HJURP to the LacO locus.

Based on these data, we propose that the CENP-C C-terminal region (aa 601–864) directly binds to HJURP and induces CENP-A incorporation at the LacO locus, independent of the Mis18 complex–HJURP pathway.

DISCUSSION

Consistent with our previous study (Hori et al., 2013), we demonstrated that tethering of the HJURP N-terminus (aa 1–400), Knl2, CENP-I, CENP-C and CENP-C C-terminus (aa 601–864) induced CENP-A incorporation at the LacO locus. HJURP is a CENP-A-specific chaperone and the Mis18 complex containing Knl2 binds to HJURP. Therefore, these two components could recruit CENP-A to the LacO locus (Fig. 7A,B). However, as it was unclear how CENP-I or the CENP-C C-terminus (aa 601–864) induces CENP-A incorporation at the LacO locus, we examined this issue in this study. We demonstrated that CENP-I or the CENP-C C-terminus (aa 601–864) induced CENP-A incorporation at the LacO locus in the absence of Knl2, whereas CENP-I did not induce CENP-A incorporation in the absence of CENP-C (Fig. 3; Fig. S4). Furthermore, the C-terminus of CENP-C associated with HJURP in the absence of Knl2 (Fig. 6C). Considering these results, we propose that the CENP-C C-terminus directly binds to HJURP to induce CENP-A incorporation, and that CENP-I recruits CENP-A via CENP-C–HJURP interaction into the LacO locus in chicken DT40 cells (Fig. 7C). The CENP-C–HJURP pathway is independent of the Knl2 (or Mis18 complex)-mediated HJURP pathway to induce CENP-A incorporation at the LacO locus.

The chicken CENP-C C-terminal region appears to bind directly to HJURP (Fig. 6). The dimer interface of the *Xenopus* CENP-C C-terminus has been proposed as the binding region for HJURP (Flores Servin et al., 2023). However, our data suggest that the chicken CENP-C dimer interface mutant (Y799A, H843A) still bound to HJURP, and that tethering of the mutant CENP-C induced CENP-A

Journal of Cell Science (2024) 137, jcs261639. doi:10.1242/jcs.261639

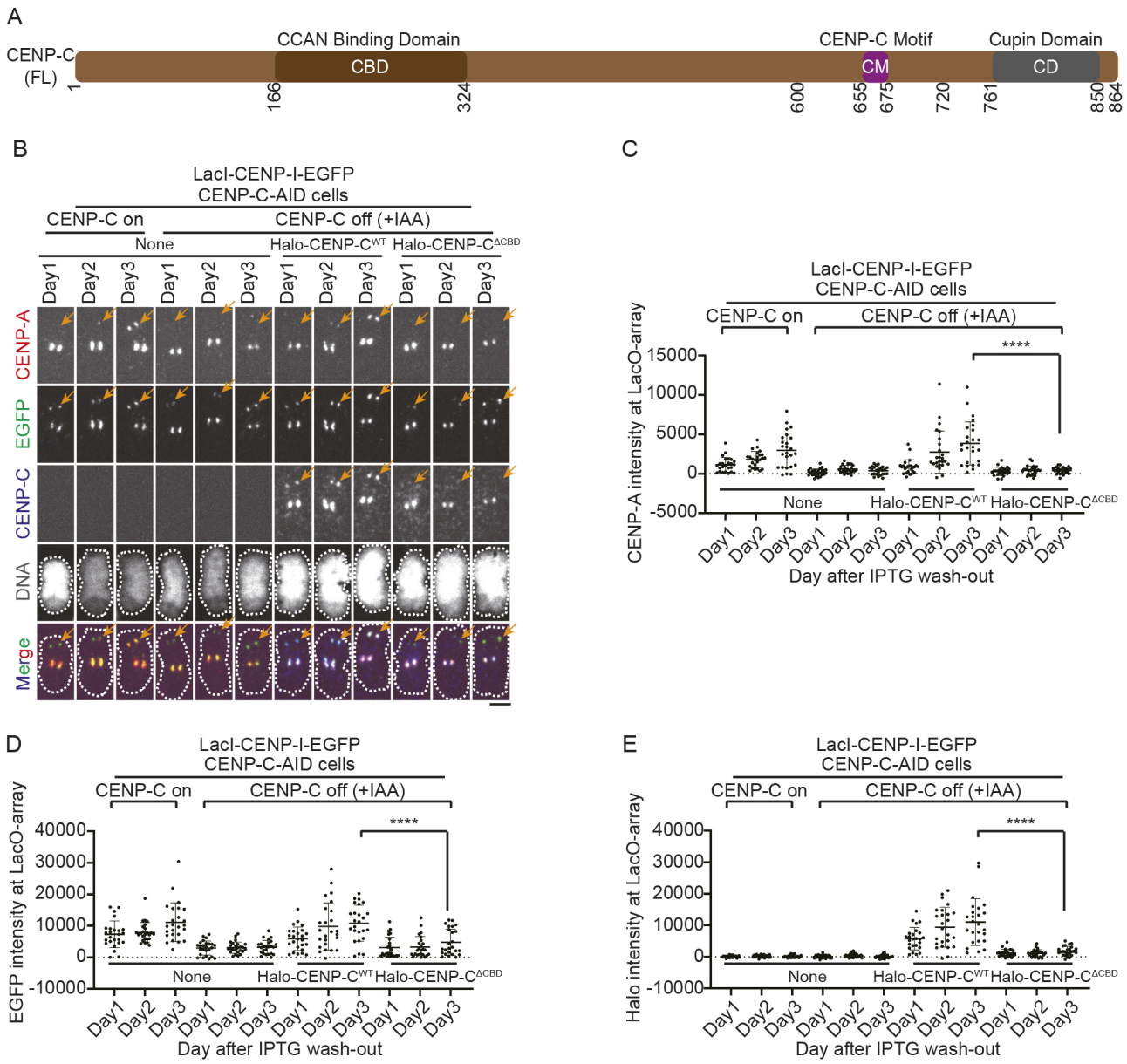

Fig. 5. The CENP-C–CENP-I interaction is essential for CENP-A incorporation at the LacO locus by CENP-I tethering. (A) Diagram depicting the domain organization of chicken full-length CENP-C (CENP-C FL). The CCAN-binding domain (CBD) spans aa 166–324, the CENP-C motif spans aa 655–675, and the Cupin domain spans aa 761–850. (B) Visualization of mScarlet-tagged CENP-A, LacI/EGFP double-fused CENP-I and Halo-tagged CENP-C^{WT} or CENP-C$^{\Delta CBD}$ at the LacO locus on chromosome Z on days 1, 2 and 3 (as per Fig. 3A) in CENP-C–AID cells expressing Halo-tagged CENP-C^{WT} or CENP-C$^{\Delta CBD}$ in the presence of IAA. Merged images with the outline of chromosome Z are shown in the bottom. The LacO locus is indicated by orange arrows. Scale bar: 2.5 µm. (C–E) The intensities (arbitrary units) of mScarlet-tagged CENP-A (C), LacI/EGFP double fused CENP-I (D) and Halo-tagged CENP-C (E) at the LacO locus in CENP-C–AID cells expressing Halo-tagged CENP-C (CENP-C^{WT} or CENP-C$^{\Delta CBD}$) in the presence of IAA are shown. The data set for CENP-C–AID cells without expression of Halo-CENP-C (None) in C is identical to that shown for LacI–CENP-I–EGFP (right-hand graph) in Fig. 3I. Bars show the mean±s.d. of the intensity values (n=25). ****P<0.0001; unpaired two-tailed t-test.

incorporation at the LacO locus in clone #2. However, CENP-A incorporation efficiency was not the same as that of wild-type CENP-C tethering (Fig. 6D,E). Although we did not directly evaluate the binding affinity of the CENP-C mutant (Y799A, H843A) to HJURP, the CENP-C mutant (Y799A, H843A) might bind to HJURP weakly, compared to wild-type CENP-C. Chicken CENP-C has two dimer interfaces, a Cupin dimer interface (Y799, H843) and a dimer hook in the pre-Cupin domain (Hara et al., 2023), each of which is sufficient for CENP-C dimer formation. However, each mutant might have a reduced dimerization activity. Stable dimer formation might be required for the proper binding of CENP-C to HJURP. Interestingly, the shorter CENP-C C-terminal region (aa 721–864), which forms a dimer, did not bind to HJURP, suggesting that CENP-C dimer formation is required for HJURP binding but is not sufficient. The detailed molecular basis of the CENP-C–HJURP interaction is an important subject for future research.

Using a similar tethering assay, Shono et al. (2015) demonstrated that tethering of CENP-C or CENP-I recruited CENP-A to a non-centromeric locus in human cells. However, the mechanism underlying CENP-A deposition by CENP-C or CENP-I in human cells might differ from that observed in chicken cells. Knl2 plays a key role in human cells, and both CENP-C and CENP-I tethering

Journal of Cell Science (2024) 137, jcs261639. doi:10.1242/jcs.261639

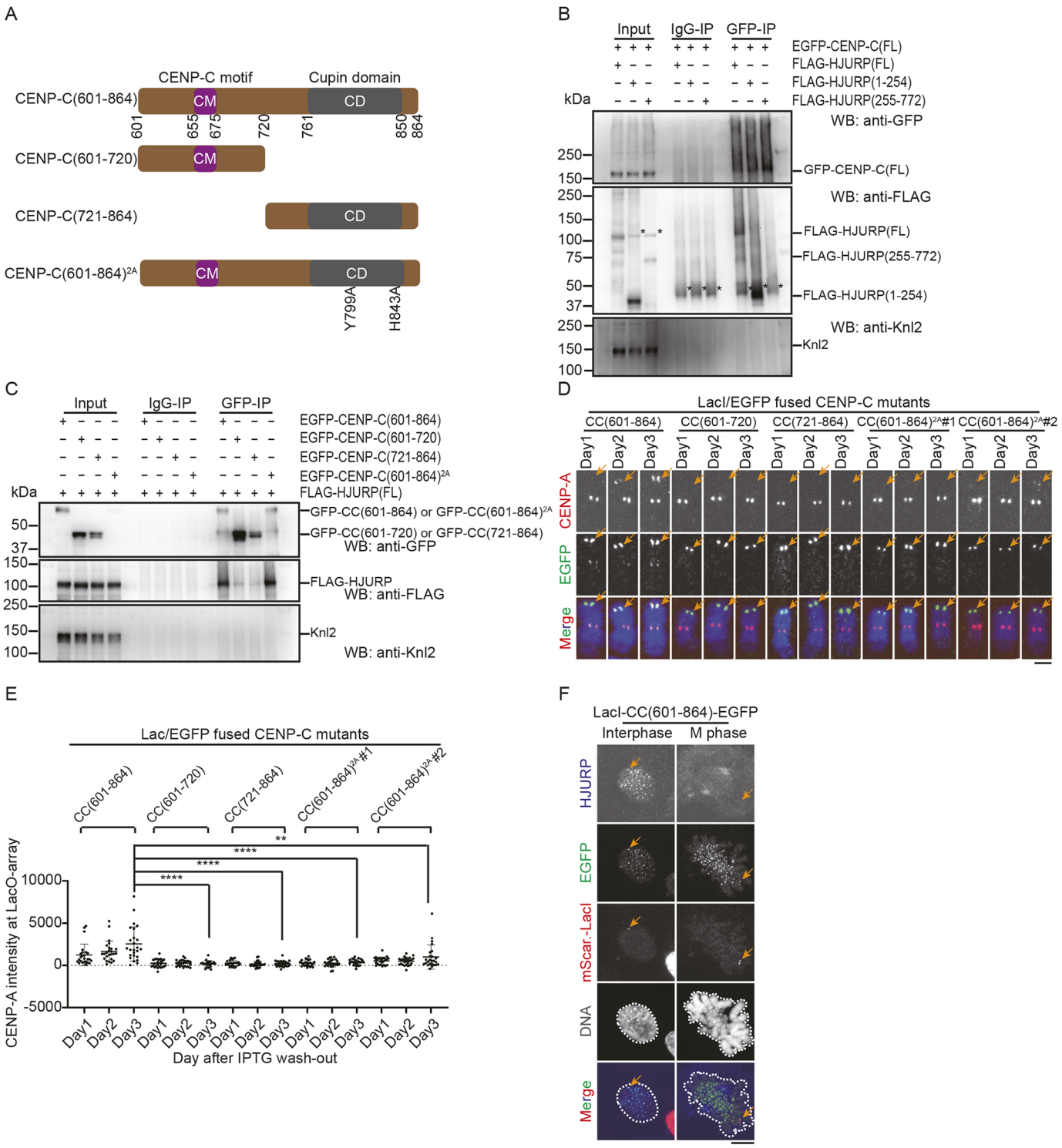

Fig. 6. See next page for legend.

reduce CENP-A recruitment after Knl2 knockdown. Furthermore, CENP-I tethering recruits CENP-A, even after CENP-C knockout in human cells. This is because CENP-I recruits Knl2 independently of CENP-C in human cells (Shono et al., 2015). Chicken Knl2 does not appear to bind to CENP-C in the G1 phase, which differs from that in human. Furthermore, chicken CENP-I might not be associated with Knl2 as our data indicate that CENP-C or CENP-I tethering induces CENP-A incorporation in Knl2-knockout chicken DT40 cells.

We also propose that chicken CENP-C directly binds to HJURP, which induces CENP-A incorporation even in Knl2-knockout cells (Fig. 7C,D). Tachiwana et al. (2015) demonstrated that human HJURP binds to human CENP-C, suggesting that the C-terminal region of human CENP-C associated with human HJURP. As this interaction is similar to that of chicken proteins, the HJURP–CENP-C interaction might be conserved between chickens and humans. Whether CENP-C–HJURP-mediated CENP-A deposition occurs in human cells is uncertain because tethering of CENP-C or CENP-I to

Journal of Cell Science (2024) 137, jcs261639. doi:10.1242/jcs.261639

Fig. 6. CENP-C binds to HJURP to induce CENP-A incorporation at the LacO locus. (A) Schematic representation illustrating the mutants of chicken CENP-C C-terminus (aa 601–864) used for co-immunoprecipitation (co-IP) experiments. The CENP-C motif-containing region encompasses aa 601–720, whereas the Cupin domain-containing region spans amino acids 721–864. CENP-C C-terminus (601–864)^{2A} mutants involved replacement of Y799 and H843 with alanine. (B) Co-IP with an anti-GFP antibody in cells transiently expressing EGFP–CENP-C (FL) and various FLAG–HJURPs (FL, aa 1–254 or aa 255–772). Immunoprecipitated samples were detected using specific antibodies against GFP, FLAG or Knl2. Asterisks (*) indicate nonspecific bands. *n*=2. (C) Co-IP with an anti-GFP antibody in cells transiently expressing various EGFP–CENP-Cs shown in A and FLAG–HJURP. Immunoprecipitated samples were detected using specific antibodies against GFP, FLAG or Knl2. *n*=2. (D) Visualization of various mScarlet-tagged CENP-A and LacI/EGFP double-fused CENP-C mutants at the LacO locus on chromosome Z on days 1, 2 and 3 (as per Fig. 2A). Merged images of mScarlet tagged CENP-A, LacI/EGFP double-fused CENP-C mutants and DAPI-stained chromosome Z are shown on the bottom. The LacO locus is indicated by orange arrows. Scale bar: 2.5 µm. (E) The intensities (arbitrary units) of mScarlet-tagged CENP-A at the LacO locus in cells expressing LacI/EGFP double-fused CENP-C mutant proteins are shown. Bars show the mean±s.d. of the intensity values. *n*=25. $^{**}P \leq 0.01$; $^{****}P<0.0001$; unpaired two-tailed *t*-test. The data set for cells with CC (601-864) is identical to that shown for LacI–CC (601-864)–EGFP in Fig. 2C,E. (F) Representative images of the localization of Halo-tagged HJURP and LacI/EGFP double-fused CENP-C C-terminal (aa 601–864) at the LacO locus. The LacO locus was identified by mScarlet–LacI, which was transiently expressed. Merged images of mScarlet–LacI, LacI/EGFP double-fused CENP-C C-terminus and Halo-tagged HJURP with outline of the nucleus are shown. The LacO locus is indicated by orange arrows. Images of interphase and mitotic cells at 4 h after removing IPTG are shown. *n*=1. Scale bar: 12 µm.

a non-centromeric locus largely reduces CENP-A assembly in Knl2-knockout cells (Shono et al., 2015). However, CENP-C–HJURP-mediated CENP-A deposition might occur to some extent in human cells.

We found that CENP-A incorporation at the LacO locus was highly activated by CENP-I tethering, when Knl2 was depleted (Fig. 3D,E; Fig. S4B,C). This hyper CENP-A incorporation did not occur by CENP-C tethering in Knl2-knockout cells. Therefore, it is possible that Knl2 might have an inhibitory role for CENP-C recruitment to CENP-I for the CENP-A incorporation activity. Therefore, CENP-C–HJURP pathway might be more active in Knl2-knockout cells. Chicken Knl2 binds to the CENP-A nucleosome and might have a structural role for CCAN organization (Ariyoshi et al., 2021; Hori et al., 2017; Jiang et al., 2023), and it is possible that Knl2 has a regulatory role for the CENP-C–CENP-I interaction. However, we need further analyses to conclude this hypothesis.

We analyzed CENP-A incorporation at a non-centromeric locus when the target protein was artificially tethered. In this artificial situation, we showed that the Knl2-independent CENP-C–HJURP interaction mediated CENP-A deposition (Fig. 7C,D). We are interested in determining the extent to which this pathway is used for CENP-A deposition on native centromeres. In our tethering assays with a combination of knockout cells, CENP-A incorporation at both the LacO locus and endogenous centromeres was reduced in HJURP-knockout cells, whereas only CENP-A incorporation at the LacO locus was compromised in either Knl2- or CENP-C-knockout cells (Fig. 3). This suggests that both the CENP-C–HJURP and Knl2–HJURP pathways work at endogenous centromeres, whereas either pathway is active at the LacO locus. However, to clarify this hypothesis, further analyses are needed.

The Knl2 (Mis18 complex)–HJURP pathway appears to be a major pathway for CENP-A deposition in chicken cells because we observed CENP-A reduction at native centromeres in Knl2- or Mis18α-knockout cells (Hori et al., 2017; Perpelescu et al., 2015). However, the reduction in levels of CENP-A at native centromeres in these knockout cells was milder than that in HJURP-knockout cells (Arimura et al., 2019; Hori et al., 2017). As Knl2 or Mis18α is essential for cell viability, the Knl2 (Mis18 complex)–HJURP is critical for new CENP-A deposition at the native centromere, and the CENP-C–HJURP pathway cannot fully compensate for defects of the Knl2 (Mis18 complex)–HJURP pathway in Knl2- or Mis18α-knockout cells. Therefore, the Knl2 (Mis18 complex)–HJURP and CENP-C–HJURP pathways might not be redundant for new CENP-A deposition into native centromeres, but each pathway might be required for CENP-A deposition and new CENP-A might be supplied from both pathways in chicken cells. The mechanisms of CENP-A deposition have been extensively characterized using *Xenopus* egg extracts (Flores Servin et al., 2023; French and Straight, 2019; French et al., 2017). Unlike in other vertebrate cells, there are two Knl2 proteins and the CENP-A deposition system is complicated in *Xenopus* cells. Nevertheless, the Knl2–HJURP and CENP-C–HJURP pathways appear to be present in the *Xenopus* system. Although each pathway is important, how these pathways contribute to new CENP-A deposition in *Xenopus* cells remains unclear. It is thus important to clarify how the Knl2–HJURP and CENP-C–HJURP pathways coordinate new CENP-A deposition at native centromeres in various experimental systems. In this study, we demonstrated the importance of the CENP-C–HJURP pathway

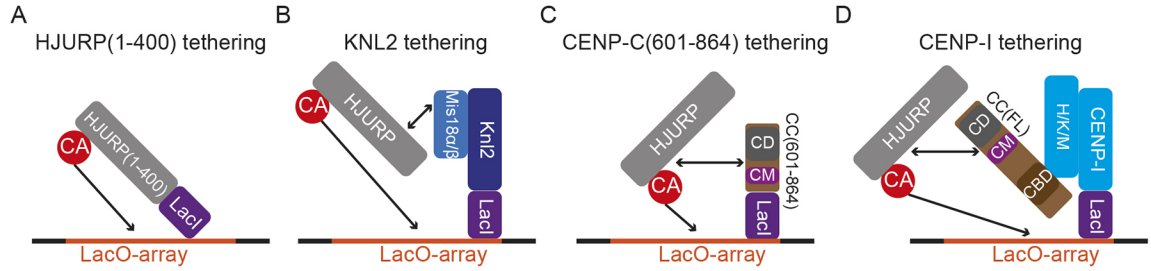

Fig. 7. Model of artificial new kinetochore formation induced by HJURP, Knl2, CENP-I or CENP-C C-terminus. We propose a model in which distinct mechanisms govern the formation of new artificial kinetochores by the induction of CENP-A (CA) to the non-centromere LacO locus. (A) As the CENP-A-specific chaperone HJURP directly binds to CENP-A via its Scm-domain (aa 1–55), HJURP tethering might directly recruit CENP-A to the LacO locus. (B) Knl2 forms the Mis18 complex with Mis18α/β; therefore, the Mis18 complex should be formed on the LacO locus by Knl2 tethering. Thus, Knl2 tethering causes CENP-A incorporation at the LacO locus via HJURP–Mis18 complex interaction. (C) The CENP-C C-terminus (aa 601–864) directly binds to HJURP, independently of the Mis18 complex, and induces CENP-A incorporation at the LacO locus via HJURP–CENP-C interaction. (D) CENP-I tethering causes formation of the CENP-H/I/K/M complex at the LacO locus, which recruits CENP-C through its CCAN-binding domain. CENP-C then recruits HJURP and induces CENP-A incorporation, similar to the process of CENP-C tethering.

Journal of Cell Science (2024) 137, jcs261639. doi:10.1242/jcs.261639

for CENP-A deposition independent of Knl2 at the LacO-mediated ectopic centromere in chicken DT40 cells, which gives us a new insight for CENP-A incorporation mechanisms.

MATERIALS AND METHODS

Plasmid construction

To generate a construct for integration of mScarlet-fused CENP-A into one β-actin allele using CRISPR/Cas9 genome editing, the mScarlet, *Gallus gallus* (gg)CENP-A, IRES2 and EcoGPT sequences were amplified using PCR and cloned into the pBluescript SK vector (Stratagene), which contains a 2-kb β-actin genome region surrounding exon 1, using In-Fusion cloning (Takara). An sgRNA sequence surrounding the start of β-actin exon 1 for targeting was designed using Cas-Designer (http://www.rgenome.net/cas-designer/) and was cloned into the pX335 plasmid (Addgene, 54233), which encodes SpCas9 nickase (D10A) (Cong et al., 2013). The final plasmid is called pX335-β-actin.

To generate the constructs for integration of EGFP/LacI double-fusion proteins into one *PGK1* allele using CRISPR/Cas9 genome editing, the following components were amplified using PCR: EGFP, LacI, protein-encoding genes [for HJURP (aa 1–400), Knl2, CENP-I^{WT}, CENP-I^{4A} (V136A, V139A, L175A, I178A), CENP-C (FL), CENP-C (aa 601–864), CENP-C (aa 601–720), CENP-C (aa 721–864) and CENP-C (aa 601–864)^{2A} (Y799A, H843A)], the SV40 promoter and the hygromycin resistance gene sequence. These components were then cloned into the pBluescript-KS(+) vector (Stratagene), which contains a 2-kb PGK1 genome region surrounding exon 1, using In-Fusion cloning. An sgRNA sequence surrounding the start of *PGK1* exon 1 for targeting was designed using Cas-Designer and was cloned into the pX335 plasmid (Cong et al., 2013). The final plasmid is called pX335-PGK1.

We generated constructs for integration of EGFP-fused CENP-I^{WT} and CENP-I^{4A} (V136A, V139A, L175A, I178A) into one *PGK1* allele using CRISPR/Cas9 genome editing. We amplified the EGFP, CENP-I^{WT} or CENP-I^{4A} (V136A, V139A, L175A, I178A) sequences, along with the SV40 promoter and the hygromycin resistance gene sequence using PCR and cloned them into the pBluescript-KS(+) vector containing the 2 kb *PGK1* genome region surrounding exon 1 using In-Fusion cloning.

To generate a construct for random integration of AID-tagged HJURP, Knl2, CENP-I, CENP-C or Mis18α along with TIR1 into DT40 cells, PCR was used to amplify the respective sequences and these were cloned into the pAID 1.1 N-T2A-Bsr (Addgene #105985) or pAID 1.1C-T2A-Bsr (Addgene #105986), which contains a TIR1 sequence and a L-histidinol dihydrochloride resistance gene sequence (Nishimura and Fukagawa, 2017) using In-Fusion cloning. The sgRNAs for targeting endogenous HJURP, Knl2, CENP-I, CENP-C and Mis18α were designed using Cas-Designer and were cloned into the pX330 plasmid (Addgene, 42330). The final plasmids are referred as pX330-HJURP, -Knl2, -CENP-I, -CENP-C and -Mis18α, respectively.

To generate constructs for random integration of Halo-tagged HJURP, CENP-C^{WT} or CENP-C$^{\Delta CBD}$ into DT40 cells, PCR was used to amplify the Halo tag and the respective protein sequence along with the SV40 promoter and a puromycin resistance gene sequence. The amplified fragments were then cloned into the pEGFP-N1 vector (Clontech), which lacks the EGFP sequence, using In-Fusion cloning. To generate constructs for transient expression of FLAG-tagged HJURP variants (FL, aa 1–254 and aa 255–772) and EGFP-tagged CENP-C variants (FL, aa 601–864, aa 601–720, aa 721–864 and aa 601–864) in DT40 cells, individual HJURP fragments were amplified by PCR and were cloned into the p3xFLAG-CMVTM-10 vector (Sigma) using In-Fusion cloning. Concurrently, PCR amplification of the CENP-C fragments was performed, followed by their insertion into the pEGFP-C1 vector (Clontech) using In-Fusion cloning.

To generate constructs for transient expression of mScarlet-tagged LacI, PCR was used to amplify the mScarlet and LacI sequences. The amplified fragments were then cloned into the pEGFP-N1 vector lacking the EGFP sequence.

Chicken DT40 cells

We used chicken DT40 CL18 cell line as the wild type (Buerstedde et al., 1990). The cells were cultured at 38.5°C in Dulbecco's modified Eagle medium (DMEM; Nakalai Tesque) supplemented with 10% fetal bovine serum (FBS; Biosera), 1% chicken serum (Gibco), and penicillin–streptomycin (referred to as DT40 culture medium).

In our previous studies (Hori et al., 2013), we created a cell line in which chromosome Z was engineered. In this cell line, a LacO array (256× repeat) was inserted at the p-arm and two LoxP sites were introduced across the native centromere of chromosome Z. To establish chromosome Z-engineered cell lines expressing EGFP–HJURP (aa 1–400)–LacI, LacI–Knl2–EGFP, LacI–CENP-I–EGFP, LacI–CENP-C (FL)–EGFP, or LacI–CENP-C (601-864)–EGFP under control of the phosphoglycerate kinase (*PGK1*) promoter, we co-transfected a plasmid encoding each LacI or EGFP fusion protein with a hygromycin resistance gene and the pX335-PGK1 plasmid encoding the sgRNA for targeting into *PGK1* gene locus and Cas9 (D10A) using electroporation. The transfected cells were selected in the DT40 culture medium containing 2.5 mg/ml hygromycin and 20 µM IPTG (for suppression of the LacI–LacO interaction). Subsequently, the cells expressing mScarlet–CENP-T or mScarlet–DsnI under the endogenous promoter were established by a CRISPR/Cas9-mediated gene-targeting method.

To establish a chromosome Z-engineered cell line expressing mScarlet–CENP-A or untagged CENP-A under control of the β-actin promoter, the plasmid encoding mScarlet-fused or untagged ggCENP-A and an EcoGPT gene was co-transfected with pX335-β-actin encoding the sgRNA targeting into the β-actin gene locus and Cas9 (D10A) using electroporation. The transfected cells were selected in the DT40 culture medium containing 25 µg/ml mycophenolic acid (TCI) and 125 µg/ml xanthine (Sigma). Using this cell line, plasmids encoding EGFP–LacI, EGFP–HJURP (aa 1–400)–LacI, LacI–Knl2–EGFP, LacI–CENP-I^{WT}–EGFP, LacI–CENP-I^{4A} (V136A, V139A, L175A, I178A)–EGFP, LacI–CENP-C (FL)–EGFP, LacI–CENP-C (aa 601–864)–EGFP, LacI–CENP-C (aa 601–720)–EGFP, LacI–CENP-C (aa 721–864)–EGFP or LacI–CENP-C (aa 601-864)^{2A} (Y799A, H843A)–EGFP with hygromycin resistance were co-transfected with pX335-PGK1. The transfected cells were selected in the DT40 culture medium containing 2.5 mg/ml hygromycin (Wako) and 20 µM IPTG (Nacalai tesque).

To create AID-based knockout for HJURP, Knl2, CENP-I, CENP-C or Mis18α in lines expressing LacI–Knl2–EGFP, LacI–CENP-I–EGFP or LacI–CENP-C (aa 601–864)–EGFP, a linearized pAID plasmid containing HJURP, Knl2, CENP-I, CENP-C or Mis18α cDNA and pX330 containing sgRNA (which targets the chicken HJURP, Knl2, CENP-I or CENP-C genome) and Cas9 gene, were co-transfected into each line (Nishimura and Fukagawa, 2017). The transfected cells were then selected in the DT40 culture medium containing 1 mg/ml L-histidinol dihydrochloride (Sigma) and 20 µM IPTG. Immunoblot analyses were performed to confirm complete replacement of the AID-fused protein with the endogenous one and to verify the successful knockout of the AID fusion protein after indole-3-acetic acid (IAA) addition. To degrade the AID-fused protein, 500 µM IAA (Sigma-Aldrich) was used. To facilitate CENP-A incorporation in the AID-based Knl-2, CENP-I- and CENP-C-knockout cells, a plasmid encoding Halo–HJURP with a puromycin resistance gene (Clontech) was transfected using electroporation. The Halo–HJURP-integrated cells were then selected in DT40 culture medium containing 0.5 µg/ml puromycin (InvivoGen) and 20 µM IPTG.

To conduct the experiments shown in Fig. 4, we generated a LacI–CENP-I^{WT}–EGFP or LacI–CENP-I^{4A} (V136A, V139A, L175A, I178A)–EGFP cell line expressing mScarlet–CENP-A and Halo–CENP-C. We introduced plasmids encoding Halo–CENP-C^{WT} with a puromycin resistance gene into each LacI–CENP-I–EGFP cell line. Cells were selected using 0.5 µg/ml puromycin and 20 µM IPTG in the DT40 culture medium.

To investigate the replacement of CENP-C by its mutant under CENP-I tethering (Fig. 5), we used the CENP-C–AID line expressing mScarlet–CENP-A and LacI–CENP-I–EGFP. To introduce plasmids encoding Halo–CENP-C^{WT} or Halo–CENP-C$^{\Delta CBD}$ with a puromycin resistance gene, electroporation was used. The resulting Halo–CENP-C^{WT}- or Halo–CENP-C$^{\Delta CBD}$- integrated cells were selected using 0.5 µg/ml puromycin and 20 µM IPTG in DT40 culture medium.

The ggCENP-I cKO cell line has been previously described (Nishihashi et al., 2002). To suppress expression of CENP-I, 2 µg/ml Tet (Sigma-

Aldrich) was added to the culture medium. To generate a cKO ggCENP-I cell line expressing either CENP-I^{WT}–EGFP or CENP-I^{4A} (V136A, V139A, L175A, I178A)–EGFP under the *PGK1* promoter, a plasmid encoding the desired protein along with a hygromycin resistance gene and pX335-PGK1 was co-transfected into the cells using electroporation. Following transfection, cells were selected in DT40 culture medium containing 2.5 mg/ml hygromycin.

Cell counting

To quantify the number of DT40 cells, a 10 µl sample of cultured medium was mixed with same volume of 0.4% (wt/vol) solution of Trypan Blue (Wako) and assessed using a Countess II automated cell counter (Thermo Fisher Scientific).

Immunoblotting

To prepare whole-cell samples, DT40 cells were harvested, washed with PBS, and suspended in 1× SDS-PAGE sampling buffer (250 mM Tris-HCl pH 6.8, 10% SDS, 50% glycerol, 5% 2-mercaptoethanol, 0.5% Bromophenol blue) (at a final concentration of 5×10^4 cells/µl) prior to sonication and heating for 5 min at 96°C. Protein samples were separated on a SuperSep Ace, 5–20% gel (Wako) and then transferred to an Immobilon-P membrane (Merck) using a HorizeBlOT system (ATTO).

The primary antibodies used in this study were as follows: rabbit anti-ggCENP-C (Fukagawa et al., 1999), rabbit anti-ggCENP-H (Fukagawa et al., 2001), rabbit anti-ggCENP-I (Nishihashi et al., 2002), rabbit anti-ggCENP-K (Okada et al., 2006), rabbit anti-ggMis18α (Hori et al., 2017), rabbit anti-ggHJURP (Perpelescu et al., 2015), rabbit anti-ggCENP-A (Hori et al., 2020), mouse anti-Halo (Promega, cat. no. G9211), rabbit anti-ggCENP-M (Okada et al., 2006), rabbit anti-ggKnl2 (Hori et al., 2017), mouse anti-FLAG (Sigma-Aldrich, cat. no. F3165), rabbit anti-GFP (MBL, cat. no. 598) and mouse anti-α-tubulin (Sigma-Aldrich, cat. no. T6199). The secondary antibodies used were HRP-conjugated anti-rabbit IgG (Jackson ImmunoResearch, cat. no. AB_2313567), HRP-conjugated anti-mouse IgG (Jackson ImmunoResearch, cat. no. AB_10015289) and HRP-conjugated anti-rabbit IgG true-blot (Rockland, cat. no. 18-8816-31). To enhance sensitivity and specificity, Signal Enhancer Hikari (Nacalai Tesque) was used for all antibodies. The membranes were blocked in 5% skim milk dissolved in TBST (20 mM Tris-HCl pH 7.5; 150 mM NaCl; 0.1% Tween-20). The membranes were incubated with all primary antibodies at 1:5000 [except for rabbit anti-ggCENP-C antibody (1:10,000); rabbit anti-ggCENP-I antibody (1:1000)] overnight at 4°C, and with secondary antibodies (1:20,000) (a dilution at 1:30,000 of secondary antibody was used when rabbit anti-ggCENP-C antibody was used as the primary antibody) for 1 h at room temperature. For antibody stripping, the membranes were incubated in stripping buffer (2% SDS, 62.5 mM Tris-HCl, 0.7% 2-mercaptoethanol) for 20 min at 60°C. The proteins that reacted with the antibodies were detected using ECL Prime (GE Healthcare) and visualized and quantified with a ChemiDoc Touch system (Bio-Rad). The acquired images were processed using Image Lab 6.1.0 (Bio-Rad) and Illustrator CC (Adobe). All raw immunoblot data are shown in Fig. S7 as 'Blot transparency'.

Immunoprecipitation

To immunoprecipitate CENP-I^{WT}–EGFP or CENP-I^{4A} (V136A, V139A, L175A, I178A)–EGFP using anti-GFP, we harvested cKO ggCENP-I cells expressing the respective constructs, which were cultured in the presence of 2 µg/ml Tet for 12 h. After cells were washed with PBS, cells were sequentially resuspended in TMS buffer (0.25 M sucrose, 10 mM Tris-HCl pH 7.5, 5 mM $MgCl_2$) and buffer A [15 mM HEPES-NaOH pH 7.4, 15 mM NaCl, 60 mM KCl, 0.34 M sucrose, 0.5 mM spermidine, 0.15 mM spermine, 1 mM dithiothreitol (DTT), and 100 ng/ml Trichostatin-A (TSA), supplemented with 1× complete EDTA-free proteinase inhibitor (Roche)]. Following centrifugation, the cell pellet was quick frozen in liquid nitrogen and suspended in buffer A again to a final density of 2×10^8 cells/ml. We then added $CaCl_2$ (final concentration 3 mM) and micrococcal nuclease (New England Biolabs) (240 gel units/ml at final concentration) and rotated the suspension at room temperature for 1 h. To stop the reaction, we added EDTA (final concentration 10 mM), followed by NaCl (300 mM at final concentration) to the digested chromatin fraction. The solubilized fraction was incubated with 10 µl Protein-G Dynabeads (Thermo Fisher Scientific) conjugated to either anti-GFP antibody (MBL, cat. no. 598, 7 µg/ml) or rabbit IgG (Sigma-Aldrich, cat. no. 12-370, 7 µg/ml) at 4°C for 2 h. The proteins precipitated with antibody-bound beads were washed with PBS three times and eluted by adding 1× sampling buffer and heating at 96°C for 5 min.

To perform immunoprecipitation of EGFP–CENP-C (FL), EGFP–CENP-C (aa 601–864), EGFP–CENP-C (aa 601–720), EGFP–CENP-C (aa 721–864) and EGFP–CENP-C (aa 601–864)^{2A}(Y799A, H843A) using anti-GFP, we transiently expressed these constructs along with FLAG–HJURP (FL), FLAG -HJURP (aa 1–254) or FLAG–HJURP (aa 255–772) in wild-type CL18 DT40 cells by transfection of plasmids (40 µg plasmids in 150 µl suspension buffer containing 3×10^6 cells). The cells were harvested 24 h after transfection, washed with PBS and suspended in lysis buffer (25 mM Tris-HCl pH 7.5, 275 mM NaCl, 5 mM $MgCl_2$, 0.1% NP40, 1 mM DTT, 0.5 µM okadaic acid, 5 mM NaF, 0.3 mM Na_3VO_4, 10 mM β-glycerophosphate-$5H_2O$, 50 U/ml Turbo-nuclease). The suspension was incubated on ice for 2 h, followed by incubation at 37°C for 10 min. After centrifugation, the solubilized fraction was incubated with anti-GFP antibody (MBL)- or control rabbit IgG (Sigma-Aldrich)-bound Protein-G Dynabeads (Thermo Fisher) at 4°C for 2 h. The proteins precipitated with antibody beads were washed thrice with lysis buffer and twice with PBS, and eluted by adding 1× SDS-PAGE sampling buffer and heating at 96°C for 5 min.

Chromosome observation

DT40 cells were cyto-spun onto glass slides. The cells were fixed with 4% paraformaldehyde in PBS for 10 min, permeabilized in 0.5% NP40 in PBS for 10 min, and stained with 1 µg/ml DAPI in PBS for 10 min. The stained samples were washed with PBS and mounted with VECTASHIELD mounting medium (Vector Laboratories).

To observe chromosome spread, DT40 cells were treated with 500 ng/ml nocodazole (Sigma) for 1 h before cyto-spinning onto glass slides. The cells were expanded in hypotonic buffer (40 mM KCl, 20 mM HEPES-NaOH pH 7.5, 0.5 mM EDTA) for 10 min at 37°C before fixation.

To detect chromosome Z, a CasFISH method was used (Deng et al., 2015). For CasFISH detection, the samples after permeabilization and before DAPI staining were washed with PBS three times and then incubated with the CasFISH reaction complex [25 nM dCas-tagged Halo conjugated with Janelia Fluor (JF) 646 (Janelia), 100 nM sgRNA for targeting a chromosome Z-specific satellite sequence, 20 mM HEPES-NaOH pH 7.4, 100 mM KCl, 5 mM $MgCl_2$, 5% glycerol, 5% BSA, 5 mM DTT, 0.5% Tween-20] for 30 min at 37°C, followed by washing with PBS three times. For detection of Halo-tagged proteins on chromosome Z, DT40 cells were stained with 200 nM JF646 (Janelia) before cyto-spinning onto glass slides.

Evaluation of efficiency for artificial centromere formation

DT40 cells containing a LacO array (256× repeat) at the end of the p-arm and LoxP sequences across the native centromere of chromosome Z and expressing each EGFP/LacI-fused target protein were used in this assay. The cells were maintained in medium containing 20 µM IPTG. IPTG was washed out with fresh medium twice at day 0. After 3 days, 4-hydroxytamoxifen (OHT, Sigma-Aldrich) was added to activate Cre recombinase. Then, native centromeres were removed by recombination between two LoxP sites. After 16 h of treatment of OHT, cells were washed with fresh medium twice and were plated into 96-well plates at several dilutions. After incubation for 8 h, zeocin (InvivoGen)-containing medium (final concentration at 1 mg/ml) was added to the plates. After further incubation for 16 h, fialuridine (Sigma)-containing medium (final concentration at 0.5 µM) was added to select surviving cells. After 2 weeks of selection, the numbers of the surviving colonies on the plates were counted.

Structure modelling

To generate a homology model of the chicken CENP-H/I/K/M complex, we used the SWISS-MODEL workspace (https://swissmodel.expasy.org/) with the cryo-electron microscopy structure of the human CENP-H/I/K/M complex (Protein Data Bank number: 7QOO) as the template. To visualize the resulting

models, we used the PyMOL Molecular Graphics System (version 2.5.2, Schrödinger) and generated ribbon presentations of the structures.

Quantification and statistical analysis

The fluorescence signal intensities of EGFP-fused proteins, mScarlet-fused proteins or Halo-tagged proteins conjugated with JF646 on the LacO locus were quantified using Imaris software (Bitplane). We measured fluorescence signals of two sister LacO arrays and obtained the mean of two sister signals. 25 LacO signals in each cell were measured and background signals in regions without signals were subtracted, respectively. Plots were made using GraphPad Prism8. In every group in each graph, means of 25 cells and s.d. are shown. Unpaired two-tailed *t*-tests were performed for corresponding groups.

Quantification of CENP-A at the LacO locus in CENP-I knockout cells were evaluated by a reversine method (Fig. 3L). AID-based CENP-I knockout cells in the presence of IPTG were treated with 500 ng/ml nocodazole and 500 µM IAA for 5 h. Then, IPTG was washed out and cells were incubated for 3 h to tether the CENP-C C-terminus into the LacO locus. Then, 1 µM reversine (Sigma) was added and incubated for 3 h. After that, only the reversine was washed out and the cells were incubated for 10 h before cyto-spinning onto glass slides. Then, CENP-A incorporation was evaluated at the LacO locus on chromosome Z.

Acknowledgements

The authors are very grateful to members of the Fukagawa Lab for the fruitful discussion. We also thank R. Fukuoka and K. Oshimo for technical assistance.

Competing interests

The authors declare no competing or financial interests.

Author contributions

Conceptualization: T.F.; Methodology: J.C., M.A.; Validation: J.C., M.A.; Formal analysis: J.C.; Investigation: J.C., T.H.; Data curation: J.C.; Writing - original draft: T.F.; Supervision: T.H., T.F.; Funding acquisition: T.F., T.H., M.A.

Funding

This work was supported by Core Research for Evolutional Science and Technology (CREST) of the Japan Science and Technology Agency (JPMJCR21E6), Japan Society for the Promotion of Science KAKENHI grants (17H06167, 20H05389, 21H05752, 22H00408 and 22H04692 to T.F., 23H02460 to T.H., and 21K06048 to M.A.).

Data availability

All relevant data can be found within the article and its supplementary information.

First Person

This article has an associated First Person interview with the first author of the paper.

Peer review history

The peer review history is available online at https://journals.biologists.com/jcs/lookup/doi/10.1242/jcs.261639.reviewer-comments.pdf

References

Allshire, R. C. and Karpen, G. H. (2008). Epigenetic regulation of centromeric chromatin: old dogs, new tricks? *Nat. Rev. Genet.* **9**, 923-937. doi:10.1038/nrg2466

Arimura, Y., Tachiwana, H., Takagi, H., Hori, T., Kimura, H., Fukagawa, T. and Kurumizaka, H. (2019). The CENP-A centromere targeting domain facilitates H4K20 monomethylation in the nucleosome by structural polymorphism. *Nat. Commun.* **10**, 576. doi:10.1038/s41467-019-08314-x

Ariyoshi, M., Makino, F., Watanabe, R., Nakagawa, R., Kato, T., Namba, K., Arimura, Y., Fujita, R., Kurumizaka, H., Okumura, E. I. et al. (2021). Cryo-EM structure of the CENP-A nucleosome in complex with phosphorylated CENP-C. *EMBO J.* **40**, e105671. doi:10.15252/embj.2020105671

Barnhart, M. C., Kuich, P. H., Stellfox, M. E., Ward, J. A., Bassett, E. A., Black, B. E. and Foltz, D. R. (2011). HJURP is a CENP-A chromatin assembly factor sufficient to form a functional de novo kinetochore. *J. Cell Biol.* **194**, 229-243. doi:10.1083/jcb.201012017

Basilico, F., Maffini, S., Weir, J. R., Prumbaum, D., Rojas, A. M., Zimniak, T., De Antoni, A., Jeganathan, S., Voss, B., van Gerwen, S. et al. (2014). The pseudo GTPase CENP-M drives human kinetochore assembly. *Elife* **3**, e02978. doi:10.7554/eLife.02978

Black, B. E. and Cleveland, D. W. (2011). Epigenetic centromere propagation and the nature of CENP-a nucleosomes. *Cell* **144**, 471-479. doi:10.1016/j.cell.2011.02.002

Buerstedde, J. M., Reynaud, C. A., Humphries, E. H., Olson, W., Ewert, D. L. and Weill, J. C. (1990). Light chain gene conversion continues at high rate in an ALV-induced cell line. *EMBO J.* **9**, 921-927. doi:10.1002/j.1460-2075.1990.tb08190.x

Cong, L., Ran, F. A., Cox, D., Lin, S., Barretto, R., Habib, N., Hsu, P. D., Wu, X., Jiang, W., Marraffini, L. A. et al. (2013). Multiplex genome engineering using CRISPR/Cas systems. *Science* **339**, 819-823. doi:10.1126/science.1231143

Dambacher, S., Deng, W., Hahn, M., Sadic, D., Frohlich, J., Nuber, A., Hoischen, C., Diekmann, S., Leonhardt, H. and Schotta, G. (2012). CENP-C facilitates the recruitment of M18BP1 to centromeric chromatin. *Nucleus* **3**, 101-110. doi:10.4161/nucl.18955

Deng, W., Shi, X., Tjian, R., Lionnet, T. and Singer, R. H. (2015). CASFISH: CRISPR/Cas9-mediated in situ labeling of genomic loci in fixed cells. *Proc. Natl. Acad. Sci. USA* **112**, 11870-11875. doi:10.1073/pnas.1515692112

Flores Servin, J. C., Brown, R. R. and Straight, A. F. (2023). Repression of CENP-A assembly in metaphase requires HJURP phosphorylation and inhibition by M18BP1. *J. Cell Biol.* **222**, e202110124. doi:10.1083/jcb.202110124

French, B. T. and Straight, A. F. (2019). CDK phosphorylation of Xenopus laevis M18BP1 promotes its metaphase centromere localization. *EMBO J.* **38**, e100093. doi:10.15252/embj.2018100093

French, B. T., Westhorpe, F. G., Limouse, C. and Straight, A. F. (2017). Xenopus laevis M18BP1 directly binds existing CENP-a nucleosomes to promote centromeric chromatin assembly. *Dev. Cell* **42**, 190-199.e10. doi:10.1016/j.devcel.2017.06.021

Fujita, Y., Hayashi, T., Kiyomitsu, T., Toyoda, Y., Kokubu, A., Obuse, C. and Yanagida, M. (2007). Priming of centromere for CENP-A recruitment by human hMis18α, hMis18β, and M18BP1. *Dev. Cell* **12**, 17-30. doi:10.1016/j.devcel.2006.11.002

Fukagawa, T. and Earnshaw, W. C. (2014). The centromere: chromatin foundation for the kinetochore machinery. *Dev. Cell* **30**, 496-508. doi:10.1016/j.devcel.2014.08.016

Fukagawa, T., Pendon, C., Morris, J. and Brown, W. (1999). CENP-C is necessary but not sufficient to induce formation of a functional centromere. *EMBO J.* **18**, 4196-4209. doi:10.1093/emboj/18.15.4196

Fukagawa, T., Mikami, Y., Nishihashi, A., Regnier, V., Haraguchi, T., Hiraoka, Y., Sugata, N., Todokoro, K., Brown, W. and Ikemura, T. (2001). CENP-H, a constitutive centromere component, is required for centromere targeting of CENP-C in vertebrate cells. *EMBO J.* **20**, 4603-4617. doi:10.1093/emboj/20.16.4603

Gascoigne, K. E., Takeuchi, K., Suzuki, A., Hori, T., Fukagawa, T. and Cheeseman, I. M. (2011). Induced ectopic kinetochore assembly bypasses the requirement for CENP-A nucleosomes. *Cell* **145**, 410-422. doi:10.1016/j.cell.2011.03.031

Guse, A., Carroll, C. W., Moree, B., Fuller, C. J. and Straight, A. F. (2011). In vitro centromere and kinetochore assembly on defined chromatin templates. *Nature* **477**, 354-358. doi:10.1038/nature10379

Hara, M., Ariyoshi, M., Sano, T., Nozawa, R. S., Shinkai, S., Onami, S., Jansen, I., Hirota, T. and Fukagawa, T. (2023). Centromere/kinetochore is assembled through CENP-C oligomerization. *Mol. Cell* **83**, 2188-2205.e13. doi:10.1016/j.molcel.2023.05.023

Hayashi, T., Fujita, Y., Iwasaki, O., Adachi, Y., Takahashi, K. and Yanagida, M. (2004). Mis16 and Mis18 are required for CENP-A loading and histone deacetylation at centromeres. *Cell* **118**, 715-729. doi:10.1016/j.cell.2004.09.002

Hori, T., Shang, W. H., Takeuchi, K. and Fukagawa, T. (2013). The CCAN recruits CENP-A to the centromere and forms the structural core for kinetochore assembly. *J. Cell Biol.* **200**, 45-60. doi:10.1083/jcb.201210106

Hori, T., Shang, W. H., Hara, M., Ariyoshi, M., Arimura, Y., Fujita, R., Kurumizaka, H. and Fukagawa, T. (2017). Association of M18BP1/KNL2 with CENP-A nucleosome is essential for centromere formation in non-mammalian vertebrates. *Dev. Cell* **42**, 181-189.e3. doi:10.1016/j.devcel.2017.06.019

Hori, T., Cao, J., Nishimura, K., Ariyoshi, M., Arimura, Y., Kurumizaka, H. and Fukagawa, T. (2020). Essentiality of CENP-A depends on its binding mode to HJURP. *Cell Rep.* **33**, 108388. doi:10.1016/j.celrep.2020.108388

Jiang, H., Ariyoshi, M., Hori, T., Watanabe, R., Makino, F., Namba, K. and Fukagawa, T. (2023). The cryo-EM structure of the CENP-A nucleosome in complex with ggKNL2. *EMBO J.* **42**, e111965. doi:10.15252/embj.2022111965

Klare, K., Weir, J. R., Basilico, F., Zimniak, T., Massimiliano, L., Ludwigs, N., Herzog, F. and Musacchio, A. (2015). CENP-C is a blueprint for constitutive centromere-associated network assembly within human kinetochores. *J. Cell Biol.* **210**, 11-22. doi:10.1083/jcb.201412028

Lacefield, S., Lau, D. T. and Murray, A. W. (2009). Recruiting a microtubule-binding complex to DNA directs chromosome segregation in budding yeast. *Nat. Cell Biol.* **11**, 1116-1120. doi:10.1038/ncb1925

Maddox, P. S., Hyndman, F., Monen, J., Oegema, K. and Desai, A. (2007). Functional genomics identifies a Myb domain-containing protein family required for assembly of CENP-A chromatin. *J. Cell Biol.* **176**, 757-763. doi:10.1083/jcb.200701065

McKinley, K. L. and Cheeseman, I. M. (2014). Polo-like kinase 1 licenses CENP-a deposition at centromeres. *Cell* **158**, 397-411. doi:10.1016/j.cell.2014.06.016

McKinley, K. L., Sekulic, N., Guo, L. Y., Tsinman, T., Black, B. E. and Cheeseman, I. M. (2015). The CENP-L-N complex forms a critical node in an integrated meshwork of interactions at the centromere-kinetochore interface. *Mol. Cell* **60**, 886-898. doi:10.1016/j.molcel.2015.10.027

Mellone, B. G. and Fachinetti, D. (2021). Diverse mechanisms of centromere specification. *Curr. Biol.* **31**, R1491-R1504. doi:10.1016/j.cub.2021.09.083

Mendiburo, M. J., Padeken, J., Fulop, S., Schepers, A. and Heun, P. (2011). Drosophila CENH3 is sufficient for centromere formation. *Science* **334**, 686-690. doi:10.1126/science.1206880

Nagpal, H., Hori, T., Furukawa, A., Sugase, K., Osakabe, A., Kurumizaka, H. and Fukagawa, T. (2015). Dynamic changes in CCAN organization through CENP-C during cell-cycle progression. *Mol. Biol. Cell* **26**, 3768-3776. doi:10.1091/mbc.E15-07-0531

Nardi, I. K., Zasadzinska, E., Stellfox, M. E., Knippler, C. M. and Foltz, D. R. (2016). Licensing of centromeric chromatin assembly through the Mis18α-Mis18β heterotetramer. *Mol. Cell* **61**, 774-787. doi:10.1016/j.molcel.2016.02.014

Nishihashi, A., Haraguchi, T., Hiraoka, Y., Ikemura, T., Regnier, V., Dodson, H., Earnshaw, W. C. and Fukagawa, T. (2002). CENP-I is essential for centromere function in vertebrate cells. *Dev. Cell* **2**, 463-476. doi:10.1016/S1534-5807(02)00144-2

Nishimura, K. and Fukagawa, T. (2017). An efficient method to generate conditional knockout cell lines for essential genes by combination of auxin-inducible degron tag and CRISPR/Cas9. *Chromosome Res.* **25**, 253-260. doi:10.1007/s10577-017-9559-7

Okada, M., Cheeseman, I. M., Hori, T., Okawa, K., McLeod, I. X., Yates, J. R., 3rd, Desai, A. and Fukagawa, T. (2006). The CENP-H-I complex is required for the efficient incorporation of newly synthesized CENP-A into centromeres. *Nat. Cell Biol.* **8**, 446-457. doi:10.1038/ncb1396

Palladino, J., Chavan, A., Sposato, A., Mason, T. D. and Mellone, B. G. (2020). Targeted de novo centromere formation in Drosophila reveals plasticity and maintenance potential of CENP-A chromatin. *Dev. Cell* **52**, 379-394.e7. doi:10.1016/j.devcel.2020.01.005

Pan, D., Klare, K., Petrovic, A., Take, A., Walstein, K., Singh, P., Rondelet, A., Bird, A. W. and Musacchio, A. (2017). CDK-regulated dimerization of M18BP1 on a Mis18 hexamer is necessary for CENP-A loading. *Elife* **6**, e23352. doi:10.7554/eLife.23352

Pan, D., Walstein, K., Take, A., Bier, D., Kaiser, N. and Musacchio, A. (2019). Mechanism of centromere recruitment of the CENP-A chaperone HJURP and its implications for centromere licensing. *Nat. Commun.* **10**, 4046. doi:10.1038/s41467-019-12019-6

Perpelescu, M., Hori, T., Toyoda, A., Misu, S., Monma, N., Ikeo, K., Obuse, C., Fujiyama, A. and Fukagawa, T. (2015). HJURP is involved in the expansion of centromeric chromatin. *Mol. Biol. Cell* **26**, 2742-2754. doi:10.1091/mbc.E15-02-0094

Pesenti, M. E., Raisch, T., Conti, D., Walstein, K., Hoffmann, I., Vogt, D., Prumbaum, D., Vetter, I. R., Raunser, S. and Musacchio, A. (2022). Structure of the human inner kinetochore CCAN complex and its significance for human centromere organization. *Mol. Cell* **82**, 2113-2131.e8. doi:10.1016/j.molcel.2022.04.027

Santaguida, S., Tighe, A., D'Alise, A. M., Taylor, S. S. and Musacchio, A. (2010). Dissecting the role of MPS1 in chromosome biorientation and the spindle checkpoint through the small molecule inhibitor reversine. *J. Cell Biol.* **190**, 73-87. doi:10.1083/jcb.201001036

Shang, W. H., Hori, T., Martins, N. M., Toyoda, A., Misu, S., Monma, N., Hiratani, I., Maeshima, K., Ikeo, K., Fujiyama, A. et al. (2013). Chromosome engineering allows the efficient isolation of vertebrate neocentromeres. *Dev. Cell* **24**, 635-648. doi:10.1016/j.devcel.2013.02.009

Shono, N., Ohzeki, J., Otake, K., Martins, N. M., Nagase, T., Kimura, H., Larionov, V., Earnshaw, W. C. and Masumoto, H. (2015). CENP-C and CENP-I are key connecting factors for kinetochore and CENP-A assembly. *J. Cell Sci.* **128**, 4572-4587. doi:10.1242/jcs.180786

Spiller, F., Medina-Pritchard, B., Abad, M. A., Wear, M. A., Molina, O., Earnshaw, W. C. and Jeyaprakash, A. A. (2017). Molecular basis for Cdk1-regulated timing of Mis18 complex assembly and CENP-A deposition. *EMBO Rep.* **18**, 894-905. doi:10.15252/embr.201643564

Subramanian, L., Medina-Pritchard, B., Barton, R., Spiller, F., Kulasegaran-Shylini, R., Radaviciute, G., Allshire, R. C. and Arockia Jeyaprakash, A. (2016). Centromere localization and function of Mis18 requires Yippee-like domain-mediated oligomerization. *EMBO Rep.* **17**, 496-507. doi:10.15252/embr.201541520

Tachiwana, H., Muller, S., Blumer, J., Klare, K., Musacchio, A. and Almouzni, G. (2015). HJURP Involvement in De Novo CenH3(CENP-A) and CENP-C Recruitment. *Cell Rep.* **11**, 22-32. doi:10.1016/j.celrep.2015.03.013

Tian, T., Chen, L., Dou, Z., Yang, Z., Gao, X., Yuan, X., Wang, C., Liu, R., Shen, Z., Gui, P. et al. (2022). Structural insights into human CCAN complex assembled onto DNA. *Cell Discov.* **8**, 90. doi:10.1038/s41421-022-00439-6

Westhorpe, F. G. and Straight, A. F. (2013). Functions of the centromere and kinetochore in chromosome segregation. *Curr. Opin. Cell Biol.* **25**, 334-340. doi:10.1016/j.ceb.2013.02.001

Yatskevich, S., Muir, K. W., Bellini, D., Zhang, Z., Yang, J., Tischer, T., Predin, M., Dendooven, T., McLaughlin, S. H. and Barford, D. (2022). Structure of the human inner kinetochore bound to a centromeric CENP-A nucleosome. *Science* **376**, 844-852. doi:10.1126/science.abn3810